DISSOLVABLE CONDUCTIVE POLYMERS FOR ELECTROCHEMICAL ENERGY STORAGE

by

Virginia M. Diaz

A thesis submitted to the faculty of
The University of Utah
in partial fulfillment of the requirements for the degree of

Master of Science

Department of Mechanical Engineering

The University of Utah

December 2017

The University of Utah Graduate School

STATEMENT OF THESIS APPROVAL

The thesis of **Virginia M. Diaz**
has been approved by the following supervisory committee members:

Roseanne Warren	, Chair	**08/11/2017** Date Approved
Shadrach J. Roundy	, Chair	**07/28/2017** Date Approved
Jiyoung Chang	, Chair	**07/28/2017** Date Approved

and by **Timothy A. Ameel**, Chair of
the Department of **Mechanical Engineering**

and by David B. Kieda, Dean of The Graduate School.

ABSTRACT

Electrochemical capacitors, or “supercapacitors”, are an electrochemical energy storage technology with high-power density and long cycle life compared to batteries. Supercapacitors have many promising applications in electric vehicles, renewable energy storage, consumer electronics, environmental sensors, biomedical implants, and grid energy storage. Conductive polymers are a material of interest for supercapacitor energy storage because of their ability to store energy by both electric double layer capacitance and “pseudocapacitance” (surface reduction-oxidation reactions). Polypyrrole is a widely used conductive polymer for supercapacitor electrodes, as well as in lithium-ion batteries. For applications in environmental sensors, transient electronics, and implantable devices, it is necessary to find supercapacitor electrode materials that are easily biodegradable. A variation of polypyrrole exhibiting methyl carboxylate side chains, which we call “MPC polymer,” is presented in this thesis as a dissolvable supercapacitor electrode. It is, to the best of our knowledge, introduced for the first time as a dissolvable electrochemical energy storage material. The supercapacitor characteristics of MPC polymer are characterized for planar electrodes as well as a nanocellulose-based composite. The MPC polymer is found to have capacitance, cycle life, and impedance characteristics comparable to state-of-the-art polypyrrole.

To my mother and sister for believing in me unconditionally.

To Moses for his infinite patience.

TABLE OF CONTENTS

LIST OF FIGURES

Figures

ACKNOWLEDGMENTS

This work wouldn't be possible without the dedication, patience and funding of my advisor and mentor Dr. Roseanne Warren who taught me all I know about energy storage and report writing and inspired me to be the best researcher I can be.

I would like to thank Nolan Ingersoll for preparing the gold wafers for this work and always offering his support.

I would also like to thank Dr. Mathieu Francoeur for offering me my first research experience. I wouldn't be presenting this thesis if it wasn't for that opportunity.

Special thanks to the Department of Mechanical Engineering at the University of Utah for funding part of this research and my degree and also to the Global Change and Sustainability Center (GCSC) at the University of Utah for partially funding my trip to the Electrochemical Society's Annual Conference at where I had the pleasure to present this research.

INTRODUCTION

Modern society depends on electrical energy for transportation, communications, built environment systems, and consumer electronics [1], [2]. For mobile and off-grid applications, electrical energy storage is needed that can support the required energy and power demands, as well as provide recharge capabilities. Electrochemical energy storage technologies, including supercapacitors, batteries, and fuel cells, can provide high efficiency electrical energy storage for a range of energy and power requirements [3]. There is currently great research interest in improving the power, energy, and recharge characteristics of electrochemical energy storage technologies, as well as developing new energy storage materials that enable expanded applications of supercapacitors, batteries, and fuel cells [4]–[7].

The focus of this research is the study of biodegradable and environmentally-friendly materials for supercapacitor energy storage. The Introduction describes the charge storage mechanisms of supercapacitors, as well as their current and future applications. Current materials research challenges specifically related to supercapacitors in environmental sensing, biomedical, and transient electronics applications are described. Finally, here it is outlined the scope of the research and the significance of this work in advancing the study of biodegradable, transient energy storage materials.

Supercapacitor Energy Storage

Supercapacitors are a form of electrochemical energy storage with high power density and low energy density compared to batteries (Figure 1.1). A supercapacitor cell consists of: metal contacts that conduct charge into and out of the supercapacitor, a separator, the electrolyte, and two electrodes (Figure 1.2) [8]. Like batteries and capacitors, multiple supercapacitor cells can be stacked or rolled to form a supercapacitor device with desired power and energy characteristics. Supercapacitors have many promising applications including: electric vehicles (especially in regenerative braking) as engine start modules for large vehicles, sustainable energy storage (i.e., solar energy storage), low power environmental wireless sensors, biomedical applications like wirelessly charged biomedical sensors and implantable wearable micro devices, as well as consumer electronics [9]–[14].

Supercapacitors store energy *via* surface charging in the form of electric double layer capacitance and/or pseudocapacitance, resulting in more rapid charging and discharging compared to batteries (which rely on bulk chemical reactions) [15]. Supercapacitors also have much longer cycle lifetimes (number of charge-discharge cycles) compared to batteries because of lower internal stress and fewer side reactions created by surface charging [16]. Commercial supercapacitors achieve over one million charge-discharge cycles, compared to several hundred cycles for lithium-ion batteries [17].

When applying a voltage difference to the supercapacitor's electrodes, mobile ions in the electrolyte form an electrochemical double layer at the electrode

surface. Energy is stored in the double layer electrostatically due to charge separation. The electrochemical double layer thickness is of the order of a few Angstroms[18]. Supercapacitors achieve high capacitances by combining electrical double layer capacitance ("EDLC") with nanoporous materials that provide high surface areas. EDLC is governed by the standard equation for capacitance [1.1]

$$C = \varepsilon \frac{A}{d} \tag{1.1}$$

where ε is the permittivity of the material, A is the electrode surface area, and d is the charge separation. Figure 1.3 compares A and d parameters for conventional capacitors and EDLC. EDLC achieve much higher capacitance values because the A/d ratio is orders of magnitude above conventional capacitors.

Pseudocapacitance is another energy storage mechanism that supercapacitors can present in combination with EDLC. Pseudocapacitance stores energy in the form of faradic chemical processes, involving electron transfer (reduction and oxidation) in the surface of the electrode [19]. Pseudocapacitance also benefits from high surface area. The charge storage attainable through pseudocapacitance is one to two orders of magnitude higher than EDLC, however pseudocapacitance generally has lower charge-discharge cycle stability [20].

Research Challenges

Research efforts on supercapacitors have historically focused on improving the energy density and power density characteristics of supercapacitors [21]–[23]. In the past several years, there has been increasing research interest in developing electrochemical energy storage technologies that use environmentally-

friendly materials and processes [24]–[26]. The life-cycle environmental impacts of energy storage technologies, including manufacturing energy and end-of-life disposal and toxicity hazards, are a growing concern for batteries, fuel cells, and electrochemical capacitors [27]. In applications such as environmental sensors and transient electronics, there is a need for energy storage materials that can safely dissolve after use and are environmentally benign [28]–[30]. For biomedical applications such as implantable health monitoring devices, energy storage materials are needed that are biocompatible and, in some applications, can safely leave the body after use [31]–[33].

A significant research challenge is developing supercapacitor electrode materials that have good energy storage characteristics (comparable to state-of-the-art materials), with the additional properties of being biocompatible, environmentally-friendly, and/or easily biodegradable [34]. In addition, supercapacitor materials should in general possess a high cycle life, which is difficult to achieve with materials that degrade or dissolve easily under mild conditions. Current state-of-the-art supercapacitor electrodes utilize robust materials, including metal oxides and carbon-based materials [35]. This benefits the mechanical properties of the material and its cycle life but does not leave room for biodegradability or solubility. A final consideration is that the electrode material, once degraded, must have environmentally benign degradation products.

Dissertation Aim and Scope

This thesis explores new materials for supercapacitors that are biocompatible and support environmentally-friendly end-of-life options (with

potential applications in transient electronics and environmental sensors), while achieving capacitance and cycle lifetimes comparable to state-of-the-art materials. The focus of this work is on the supercapacitor electrode material. Research efforts are also needed to develop biocompatible and environmentally-friendly materials for the supercapacitor cell packaging, electrolyte, and electrical components, however, these components are beyond the scope of this thesis [24]. As a preliminary test of biodegradability, this work tests the ability of the proposed electrode materials to dissolve in mild aqueous conditions. Future research is needed to test the chemical compatibility of the electrode materials and dissolution products for environmental and biomedical applications [36].

Significance of the Study

This work presents for the first time a repeating polymer of methyl 1H-pyrrole-3- carboxylate monomer (“MPC polymer”) as a supercapacitor energy storage material, and its ability to dissolve in a mild aqueous environment. This work is, to the best of our knowledge, the first demonstration of electrochemical energy storage using a dissolvable conducting polymer derivative, and thus represents an important contribution to the field of transient, biocompatible energy storage materials. Additionally, the dissolvable polymer is deposited on a soluble highly porous substrate based on cellulose. In addition to their use as supercapacitor electrode materials, conducting polymers have also found promising application in enhancing the performance of lithium-ion batteries and as structural materials in biomedical implants [37]–[40]. The results of this study therefore have potential impacts in the battery research field and conducting

polymer-based biomedical devices generally. Finally, we recognize that achieving fully biodegradable, environmentally-friendly energy storage devices for widespread applications in renewable energy storage and electric vehicles is a challenging task; this work contributes to this aim in a small capacity with hopes of inspiring future research on sustainable energy storage materials.

Overview

Methods describes the methods used to characterize energy storage and material properties of the supercapacitor electrodes developed in this work. The aim of Methods is to introduce the reader to the metrics and tests that will be referenced throughout this study. The third section describes the fabrication and testing of supercapacitor electrodes using MPC polymer on a planar current collector. The aim of the third section is to demonstrate the solubility of MPC polymer in mild aqueous conditions, and show that its electrochemical energy storage capacity is comparable to that of polypyrrole. The fourth section explores a design that puts together the dissolvable conductive polymer (MPC polymer) and a nanocellulose-based dissolvable substrate to enhance the surface area. Last, the last chapter summarizes the main accomplishments and contributions of this thesis to the energy storage field, and suggests next steps for future work.

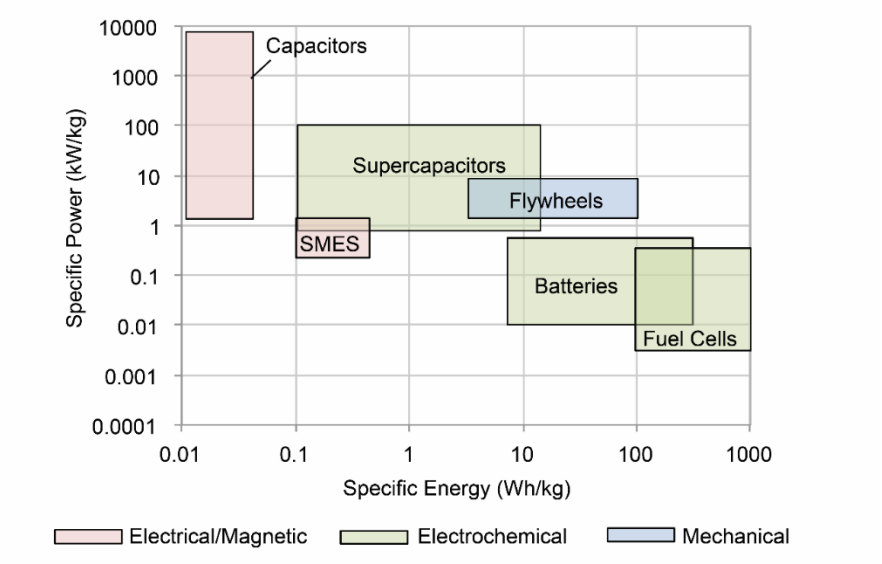

Figure1.1 Ragone plot. Comparing specific energy and specific power for different energy storage technologies [41].

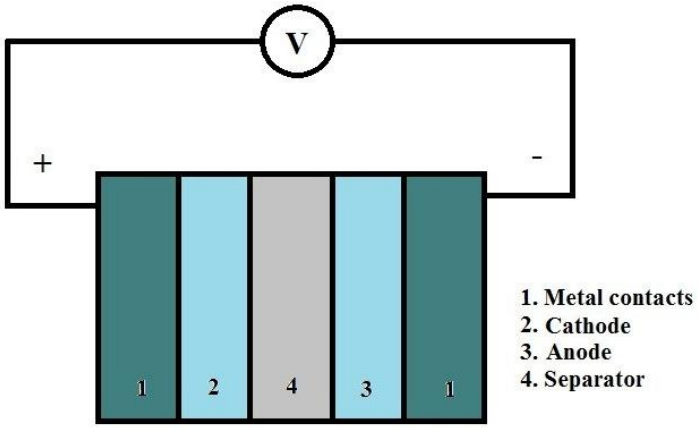

Figure 1.2 Schematic of a supercapacitor cell [8].

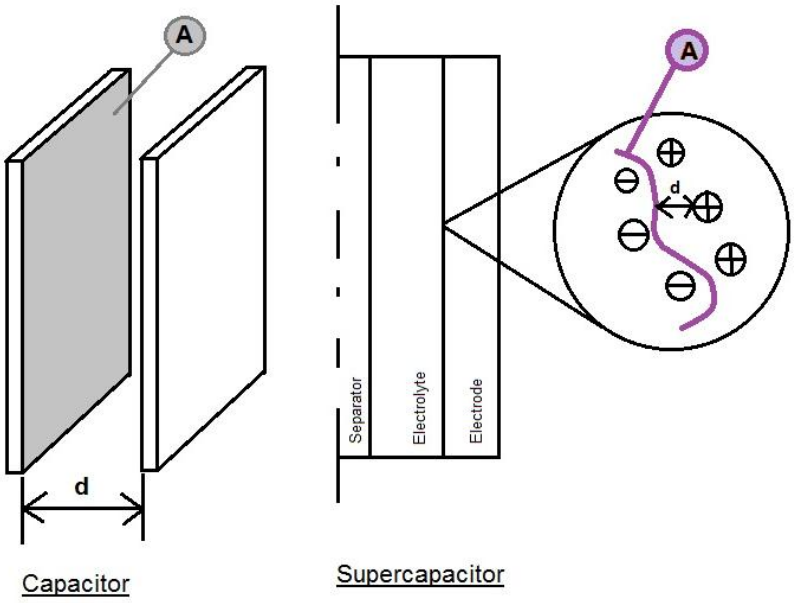

Figure 1.3 Representation of “A” and “d” for capacitors and supercapacitors.

METHODS

The previous chapter introduced the importance of developing biodegradable, environmentally-friendly supercapacitor electrode materials for applications in transient electronics, biomedical devices, and environmental sensors. Introduction also reviewed supercapacitor structure and energy storage mechanisms, as well as the thesis aim and scope. Methods introduces supercapacitor energy storage metrics and performance testing methods. These methods will form the basis for comparing and evaluating the performance of new electrode materials presented in the third and fourth sections.

Electrochemical Testing Set-Up: Three-Electrode Cell

Electrochemical measurements reported in sections third and fourth were conducted using a three-electrode electrochemical test cell. A three-electrode cell was also used to electropolymerize polypyrrole (PPY) and the MPC polymer in the third section. A three-electrode cell consists of a: working electrode (WE), reference electrode (RE) and counter electrode (CE) (Figure 2.1). The WE is where the reaction of interest occurs. In our studies, the WE is the electrodeposition substrate or supercapacitor electrode to be characterized. The RE is an electrochemical system with constant composition that provides a standard electrochemical potential against which the WE potential is measured [42].

An Ag/Ag^{+} RE (standard for nonaqueous electrolyte systems) was used in this work. The CE passes current from the WE to complete the electrochemical circuit. Large surface area Pt wire was used as the CE to provide good conductivity and not limit the WE reaction. A Gamry Interface 1000E potentiostat was used for all electrochemistry testing in this work.

Supercapacitor Performance Measurements

Three electrochemical measurements were used to characterize the energy storage properties of supercapacitor electrodes in this work: cyclic voltammetry, chronoamperometry, and electrochemical impedance spectroscopy (EIS). The following section describe these three measurement techniques, and how they were used to determine key supercapacitor electrode performance parameters.

Cyclic Voltammetry

During CV measurements, the potential applied to the WE is cycled linearly between two set potentials at a specified rate and the resulting current is measured. Figure 2.2 illustrates theoretically “ideal” and typical “nonideal” supercapacitor CV curves. The theoretically ideal CV behavior results from the characteristic equation of a capacitor:

$$\frac{dE(t)}{dt} = \frac{I(t)}{C} \tag{2.1}$$

For ideal supercapacitor electrodes with constant capacitance, charging and discharging currents are constant. However, the lack of perfect conductivity, slower redox reactions, and irreversible side reactions can result in nonideal behavior.

The capacitance of a supercapacitor electrode is proportional to the area of the CV curve, and can be calculated using the following equation:

$$C = \int_{E_1}^{E_2} i(E)dE/2(E_2 - E_1)mv \quad (2.2)$$

where *i(E)* is the instantaneous current, *(E_2-E_1)* is the CV potential window, *m* is the mass of the individual sample, and *v* is the potential scan rate. The integral of the instantaneous current over the potential window is the total voltammetric charge.

Repeated CV measurements can be used to evaluate the cycle life of a supercapacitor electrode. Typical cycle life tests consist of several thousand repeated charge-discharge cycles, from which the percentage change in the capacitance of the electrode can be evaluated [43]. Changes in the shape of the CV curve during repeated cycling can also be used to assess electrode irreversibilities and degradation over time.

Chronoamperometry

Chronoamperometry measures current response versus time when a step voltage is applied to the working electrode. Chronoamperometry can be used to evaluate the relative contributions of faradic current (I_{Far}) and double layer capacitive current (I_{cap}) to the supercapacitor total charge storage. Double layer capacitive current decays exponentially with time after a step change in potential:

$$I_{cap} \propto e^{-kt} \quad (2.3)$$

based on the general equation for the charge on a capacitor [42]. Faradic capacitive current is governed by diffusion of ions to the electrode-electrolyte interface (assuming the reaction rate constant is large), as specified by the Cottrell

Equation [42]:

$$I_{far} \propto t^{-1/2} \tag{2.4}$$

In the third section, the above equations are fit to experimental chronoamperometry results to compare the charging mechanisms of PPY and MPC polymer. Like CV measurements, repeated chronoamperometry can also be used to assess the stability of the supercapacitor material.

Electrochemical Impedance Spectroscopy

Electrochemical impedance spectroscopy (EIS) is a powerful and complex tool for understanding the mechanisms of resistance, capacitance, diffusion, and reaction kinetics that govern supercapacitor charge storage. EIS applies an AC voltage at varying frequencies between the WE and RE to measure the complex impedance of the electrochemical cell. The applied AC voltage is small (≤ 10 mV) such that the system can be assumed to be at steady state. [42]

An equivalent circuit model can be fit to EIS measurements to provide information on the series resistance of the cell, the supercapacitor electrode charge transfer resistance, the diffusion of electrolyte ions, and the cell double layer capacitance. Figure 2.3 presents a schematic of a Nyquist plot (imaginary vs. real impedance measured over a range of AC frequencies); (Figure 2.4a) and the corresponding equivalent circuit model (Figure 2.4b) of an ideal supercapacitor electrode. R_s represents the equivalent series resistance of the electrochemical cell (including wiring, the electrodes, and the electrolyte). R_{ct} is the electrode charge transfer resistance. CPE represents the electric double layer capacitance C_d, according to the equation:

$$Z_{CPE} = \frac{1}{(j\omega)^{\alpha} C_d} \tag{2.5}$$

where α accounts for nonideal behavior. The parameter *W* is known as the Warburg impedance, and represents diffusion polarization. *W* defines the slope of the Nyquist plot at low frequencies. “RE” and “WE” refer to the reference and working electrodes, respectively. In this work, Gamry’s Echem Analyst™ software was used to fit the equivalent circuit model in Figure 2.3b to measured impedance values. The circuit in Figure 2.3b is referred to as “CPE with diffusion” in Echem Analyst™. Echem Analyst™ provides a measure of the “goodness of fit” of the equivalent circuit model parameters so that the accuracy of the fit can be evaluated (see third section).

Summary

This chapter visited the methods for material characterization and supercapacitor metrics: CV for capacitance measurement and life cycle testing, chronoamperometry to characterize the charging mechanism, and EIS for impedance characterization. Understanding these three methods, the reader will follow the analysis performed on the MPC polymer in the third and fourth sections.

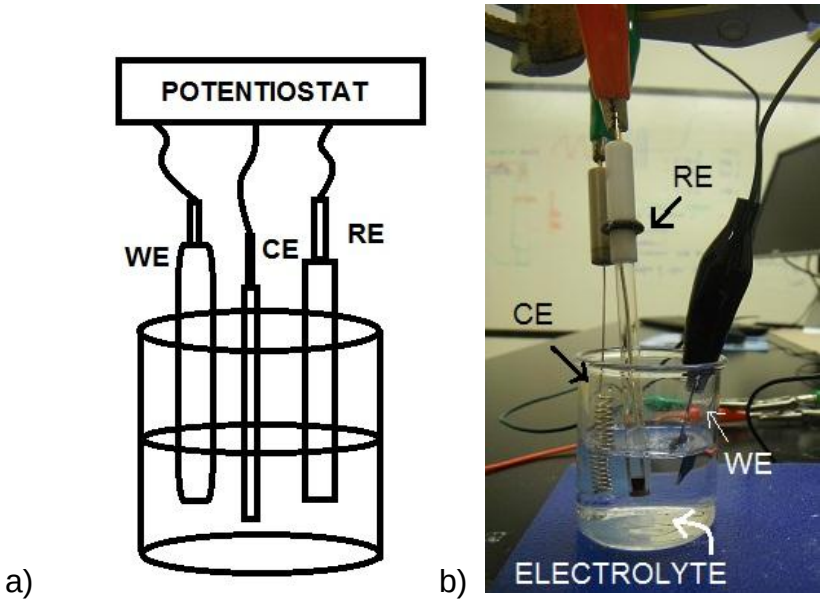

Figure 2.1 Three-electrode cell schematic. a) Simplified figure of the three-electrode test set-up. b) Labeled 3-electrode cell used in our experiments.

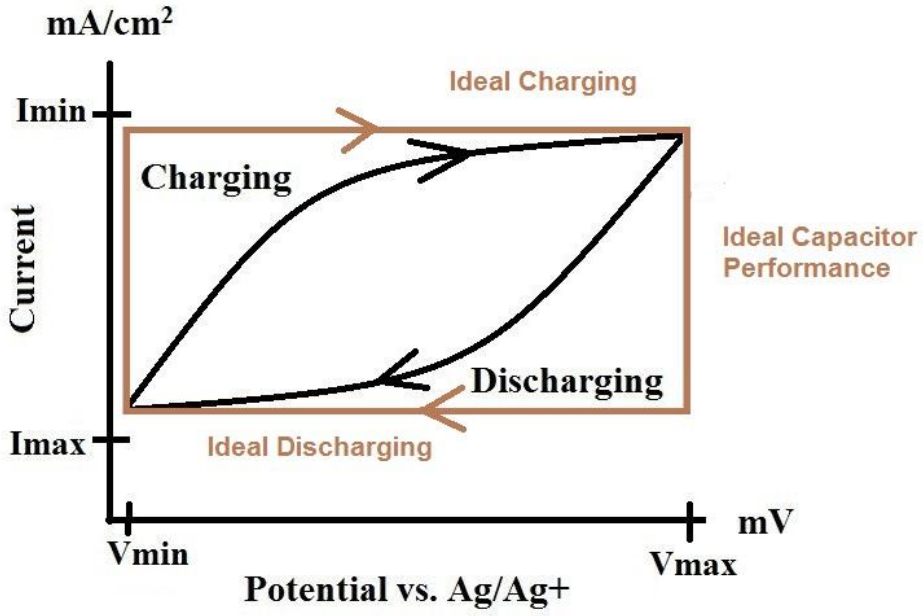

Figure 2.2 Ideal CV schematic. Current vs. potential curve for a supercapacitor electrode undergoing a CV test, showing both “ideal” and “nonideal” capacitive behavior.

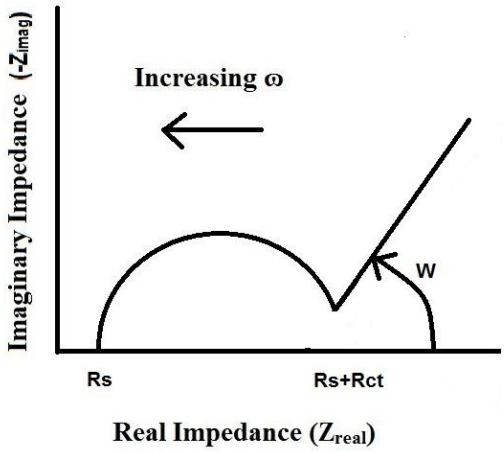

a)

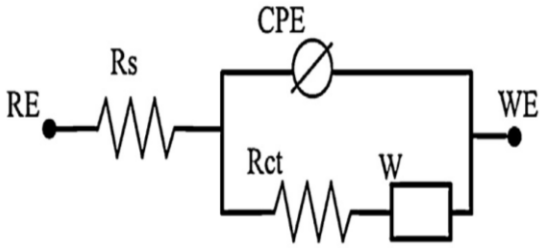

b)

Figure 2.3 Ideal EIS parameters representation. a) Representation of an ideal Nyquist plot for a supercapacitor electrode. b) Equivalent circuit model ("CPE with diffusion") used to fit EIS measurements.

PLANAR MPC POLYMER SUPERCAPACITOR ELECTRODES: SYNTHESIS AND ELECTROCHEMICAL TESTING

As described in Introduction, there is a need to develop environmentally-friendly, biodegradable materials for supercapacitor electrodes. This part introduces for the first time a repeating polymer of methyl 1 H-pyrrole-3-carboxylate monomer ("MPC polymer") as a dissolvable electrode material for electrochemical energy storage. MPC polymer—a derivative of state-of-the-art electrode material polypyrrole (PPY)—is electrochemically deposited on a planar substrate to measure its supercapacitor charge storage characteristics. MPC polymer is found to have capacitance, cycle life, and impedance characteristics comparable to PPY, while being dissolvable in mild aqueous conditions.

This part begins with a review of previous work on biodegradable supercapacitor materials and applications of PPY. The fundamentals of conductive polymers (CPs) and their supercapacitor charge storage mechanism are then presented. The MPC polymer synthesis method is described, and supercapacitor electrochemical measurements compared with planar PPY electrodes to characterize MPC polymer as a conductive polymer for electrochemical energy storage. Finally, both MPC polymer and PPY are tested for their ability to dissolve in mild aqueous conditions.

Literature Review: Biodegradable Electrochemical Energy Storage Materials and PPY-based Supercapacitors

Research efforts on biodegradable, dissolvable, and/or environmentally-friendly supercapacitors to date have largely focused on biodegradable polymer electrolytes; there has been significantly less previous work on biodegradable or dissolvable supercapacitor electrode materials [44]–[46]. Wang *et al.* proposed a "food-materials-based" edible supercapacitor using activated charcoal on gold leaf as the electrode material, a seaweed separator, and Gatorade electrolyte [47]. The resulting supercapacitor utilizes only double layer capacitance, resulting in a low capacitance value of 80 F/g. Chen *et al.* claimed a "biodegradable" and "biocompatible" activated wood carbon with MnO_2 nanosheets, however, the biodegradable aspect of the electrode is not tested or evaluated [48]. Several researchers have reported edible and/or biodegradable batteries, including a melanin-based sodium-ion battery and biodegradable metal foil-based primary batteries [49], [50]. To the best of our knowledge, a fully dissolvable supercapacitor electrode with faradaic capacitance (pseudocapacitance) has not yet been demonstrated.

PPY is a widely studied CP material for supercapacitor electrodes because of its ease of synthesis, good charge storage reversibility, high faradaic capacitance, and redox potentials within the electrochemical stability of common electrolytes [51]–[56]. In addition to its use as a supercapacitor electrode material, PPY is used in a wide range of fields, including environmental sensing and biomedical applications. V. Syritski *et al.* used PPY to coat environmental QCM

sensors [57]. Qaisar Ameer *et al.* utilized PPY to produce electronic noses for environmental analysis [58], where PPY's change in conductivity in the presence of certain gases help detect substances in the air. In biomedical applications, PPY is used often for tissue engineering because it is electrically responsive and thermally stable [59], [60]. For the same reasons, it is used in biomonitoring devices, including DNA monitoring by Kavita Aora *et al.* [61], glucose biosensors by Minni Singh *et al*. as well as implantable devices [47], [65], [63]–[65].

PPY is often cited as an "environmentally-friendly" material, however, it is not itself biodegradable, dissolvable or erodible [54][66]. Instead, PPY is often combined with biodegradable materials (including cellulose or poly-L-lactic acid). In these studies, quantities of PPY must be minimized to reduce accumulation and resulting harmful effects [67].

An important first step in the advancement of environmentally friendly, biodegradable energy storage devices is developing materials that break down under mild conditions. Several researchers have investigated methods to make CPs that are easily dissolvable (or "erodible"). Potential modifications to PPY to make it biocompatible include using a CP-based oligomer structure, however these materials are difficult and expensive to synthesize [68], [69]. Zelikin *et al.* developed an erodible version of PPY using side-chain moieties to reduce polymer crosslinking. The resulting polymer was found to be dissolvable in aqueous solution at 37 ^{o}C and pH 8.2 [70]. To the best of our knowledge, this approach has not been used or tested previously to develop biodegradable electrochemical energy storage materials.

Conductive Polymer Doping and Energy Storage

CPs store electrochemical energy as supercapacitors by both double layer capacitance and pseudocapacitance (Figure 3.1), with pseudocapacitance being the main contribution to the total energy storage. The pseudocapacitance mechanism of CPs is based on reversible reduction and oxidation of the polymer. Dopant ions move in and out of the polymer matrix as the polymer is reduced or oxidized to compensate for the net charge. Equation 3.1 represents the reversible oxidation-reduction reaction that makes PPY a pseudocapacitive material. Figure 3.2 provides a schematic illustration of dopant ion movement during oxidation-reduction reactions in the main chain of the polymer. Faradic reactions are slower than capacitive processes due to the fact that ion transport is a slower process than electrostatic adsorption [71]:

$$PPY^{+} \text{ (Oxidized)} + e^{-} \leftrightarrow PPY^{o} \text{ (Reduced)} \qquad (3.1)$$

The polymerization and doping method selected strongly affects the supercapacitor performance of CPs [72]. The two main polymerization and *in-situ* doping techniques are: 1) electrochemical polymerization proceeding by an electrochemical potential applied to the deposition substrate (dopant ions diffuse from the electrolyte out of or into the conjugated polymer to compensate the charge during polymerization), and 2) chemical polymerization in which a chemical oxidizing agent is used to trigger polymerization [72]. This part focuses on the polymerization and characterization of the MPC Polymer as an electrode material for electrochemical energy storage. Electrochemical doping has been selected due to its simplicity, good control over the polymer deposition by

adjusting the deposition current and time, and ability to extract important information on the polymer deposition process as it is performed such as the amount of charge used in the polymerization [72]. Electropolymerization with electrochemical doping uses a three-electrode cell performing chronopotentiometry (constant applied current). During electropolymerization, the corresponding monomer is oxidized from solution and deposited at the working electrode. Negative ions from the electrolyte solution diffuse into the as-depositing polymer chain to compensate the net positive charge, resulting in *in-situ* doping during electropolymerization. Figure 3.3 shows the electropolymerization and electrochemical doping process for PPY.

Dissolvable Supercapacitor Electrode Concept

This work proposes for the first time a repeating polymer of methyl 1*H*-pyrrole-3-carboxylate monomer ("MPC polymer") as a supercapacitor energy storage material that can dissolve in mild aqueous conditions. Figure 3.4 compares the structure of MPC polymer and PPY. The MPC polymer has an identical main chain structure to PPY, with the addition of methyl carboxylate side groups in the third carbon position. Similar supercapacitor performance is expected for the MPC polymer and PPY given that the conjugated structure is the same for both polymers. Polymer chains cross-link through van der Waals forces that depend on the alignment of, and separation between, polymer chains. Given the compact structure of PPY compared to MPC polymer, the van der Waals forces that keep the different chains of PPY together are expected to be stronger than those of MPC polymer. Following the approach proposed by Zelikin *et al*., it is expected that the

side chains on MPC polymer will reduce crosslinking, enabling the dissolution of the polymer under mild conditions [70]. Furthermore, the polar structure of MPC polymer is expected to enable dissolution in aqueous environments.

PPY and MPC Polymer Electrode Synthesis

PPY and the MPC polymer were electrodeposited onto a conductive, planar substrate from a solution containing the dopant and the monomer, according to the standard procedure [73] The substrate selected is a Si wafer with 10 nm Cr and 50 nm Au coating deposited by sputtering. Au was chosen as an ideal electrode surface material to simplify the electropolymerization process, since it is electrochemically inert within the potentials required for polymer electrodeposition and it is highly conductive. All chemicals were used as received from Sigma Aldrich. An Ag/Ag^+ RE (a standard nonaqueous RE) and Pt wire CE were used in the electrodeposition of both polymers (Figure 3.5).

For PPY electrodeposition, 0.1 M tetrabutylammonium hexafluorophosphate ($TBAPF_6$) dopant with 0.1 M pyrrole, 10^{-5} M HCl, and 1 mM water in acetonitrile was used as the electrodeposition solution. The Au deposition substrate was immersed in the solution and a current of 0.007 mA/s was applied. A substrate of 1 cm^2 achieves a full deposition after 1100 s. Full deposition is considered by visual inspection when the gold layer doesn't show through the PPY and the PPY layer is thick enough to take reliable measurements, which was confirmed by trial-and-error. Pyrrole is a very sensitive monomer and reacts with air, so it must be kept and handled under an inert atmosphere until it is polymerized into PPY. Argon gas was used to create the inert atmosphere, and

continuous Ar bubbling was used during the electrodeposition process.

Because the MPC polymer is expected to polymerize the same way PPY does, assembling through the first and fourth carbon links, the same monomeric solution and current/time were used at first but no positive results were obtained. After some experimentation, it was found that no water is required and that the addition of HCl inhibits MPC polymerization. MPC polymer deposition was found to occur at pH of 6.4 (vs. 7.2 for PPY). The current necessary for the MPC polymerization to occur was found to be 0.01 mA/s for 1500 s, indicating that the MPC polymer does not electrochemically polymerize as easily as PPY.

Supercapacitor Electrode Performance

Planar samples of PPY and MPC polymer were tested as supercapacitor electrodes using the electrochemical techniques explained in Methods: cyclic voltammetry (CV), chronoamperometry, and electrochemical impedance spectroscopy (EIS). Repeated CV measurements were used for a cycle life comparison.

Cyclic Voltammetry

CV measurements were used to determine the capacitance of planar PPY and MPC polymer electrodes. For each measurement, a 1 cm^2 polymer-coated electrode was placed in a three-electrode cell set-up inside a beaker with 0.1 M $TBAPF_6$ in acetonitrile. The RE was Ag/Ag^+ and a coiled Pt electrode was used as the CE to provide a large enough surface area so the WE reaction was not limited. The scan speed was 100 mV/s.

Figure 3.6 compares CV measurements for both polymers. PPY, in yellow, presents a more rectangular shaped CV curve while the MPC polymer, in gray, presents a pronounced belly around 0.4 V for cathodic current flow (polymer oxidation). These results suggest that PPY is a more capacitive material than MPC polymer and presents a behavior closer to an ideal supercapacitor. The potential range for the CV measurements is -0.2 to 0.5 V vs. Ag/Ag^{+}. This is within the common voltage ranges for PPY [74]; additionally, when trying to go over 0.8 V while charging (anodic current flow), a pronounced peak is observed with the MPC polymer, likely indicating polymer degradation or other electrode instabilities.

For the planar supercapacitor electrodes synthesized in this part, current was measured per cm^2 of sample area; capacitance is therefore calculated for both materials in F/cm^2. The capacitance, following the capacitance equation, is found to be 1.96 mF/cm^2 for PPY and 0.87 mF/cm^2 for the MPC polymer. This is consistent with reported capacitances for PPY, which are in the range of 1 to 8 mF/cm^2 [75] (note that comparing capacitance results from different literature sources is complicated due to variations in electrolyte, cell set-up, and other testing conditions). A limitation of measuring capacitance per planar surface area is that differences in electrode (polymer) thickness and micro-surface area could affect the capacitance comparisons. Despite this limitation, capacitance per planar electrode area is widely used in the literature [76]–[78]. Furthermore, the objective of this stage's investigation is to obtain an order-of-magnitude comparison of MPC polymer and PPY to assess the viability of MPC polymer as a supercapacitor material (section four provides a more accurate F/g comparison of PPY- and MPC-

nanocellulose electrodes). Through the future optimization of MPC polymer deposition parameters and the monomeric solution composition, it is expected that the capacitance of MPC polymer could be improved from the initial results reported here. This test was taken on three different samples and the shape prevailed, at the same time, when performing the life cycle test, 2,000 cycles were performed and the shape didn't change either.

Chronoamperometry

Figure 3.7 shows chronoamperometry measurements of PPY and MPC polymer for 10 charge-discharge cycles between 0 and 0.5 V. As explained in Methods, with this experiment we aim to characterize the charging and discharging mechanism through curve fitting approximations of the experimental chronoamperometry current profiles. Excel 2016 was used to find the proportionality and exponential constants that best fit the capacitive (double layer capacitance) and/or faradic (redox-based capacitance) currents in the charge and discharge mechanisms. Figure 3.7b-e show the capacitive and faradic fits obtained for PPY and MPC polymer electrodes (anodic and cathodic currents). Table 3.1 presents the capacitive and faradic fit equations used to achieve the fit for both behaviors. The current convention used is that specified by the Gamry potentiostat software: positive current is defined as electrons entering the working electrode (anodic current, or polymer reduction: $MPC^{+} + e^{-} \rightarrow MPC^{0}$); negative current is electrons leaving the working electrode (cathodic current, or polymer oxidation: $MPC^{0} \rightarrow MPC^{+} + e^{-}$). Anodic current is referred to as the electrode "charging", and cathodic current as "discharging" (consistent with CV curves).

Figure 3.7b and 3.7c provide curve fits for anodic (positive; electrode charging) and cathodic (negative; electrode discharging) current measurements, respectively, for PPY electrodes. For both cathodic and anodic currents, the first part of the curve corresponds with a capacitive fit while the end of the curve corresponds with a faradic fit. This result is consistent with the fact that the capacitive (electrostatic) charge/discharge mechanism occurs faster than faradic (chemical) reduction/oxidation reactions. Anodic and cathodic current profiles for PPY are highly symmetric, as shown by comparing capacitive and faradic fit equations in Table 3.1, and as confirmed previously by CV measurements (Figure 3.6)).

MPC polymer chronoamperometry measurements show notable asymmetry between anodic (Figure 3.7d) and cathodic (Figure 3.7e) currents. MPC polymer cathodic current is well fit by a faradic current model. This result confirms that polymer reduction-oxidation mechanisms are the main contribution to the MPC polymer supercapacitor charge storage mechanism. MPC polymer anodic current at first follows a faradic current model, but deviates after approximately 2 s of charging when the experimental current begins increasing. The observed deviation in anodic current from the faradic model is likely due to side reactions or irreversibilities. We note in Figure 3.7a that the MPC polymer electrode anodic current deviation increases with each successive cycle, suggesting irreversible changes in the electrode with repeated charge-discharge cycling. Further investigation is needed to identify potential causes of anodic current deviations in MPC polymer, as the observed nonconformances.

Electrochemical Impedance Spectroscopy

EIS measurements were conducted for both PPY and MPC polymer electrodes. An AC voltage of 10 mV was applied over a frequency range of 100 Hz-100 kHz with no DC bias. Both polymers were subjected to the same test conditions. Figure 3.8 compares Nyquist plots of real vs. imaginary impedance for PPY and MPC polymer electrodes. The two CP electrodes exhibit similar Nyquist curves, with relatively low impedance values compared to literature results for PPY electrodes (likely because of the Au substrate) [74].

A “Constant Phase Element (“CPE”) with Diffusion” equivalent circuit model was fit to the EIS results using Gamry’s Echem Analyst software. Table 3.2 summarizes the resulting equivalent circuit values (model fit curves are also shown in Figure 3.8). It should be noted that these results are meant to be compared qualitatively with the purpose of assessing the electrochemical energy storage characteristics of MPC polymer *vs.* PPY (e.g., an order-of-magnitude increase in CPE value indicates greater double layer capacitance, but does not necessary correspond to exactly a 10x increase). The following comparisons between MPC polymer and PPY are noted:

- **Series resistance**. As shown in Table 3.2, MPC polymer and PPY electrodes have similar values of series resistance (R_s) (1.3 Ω vs. 2.5 Ω, respectively), as calculated by the CPE with diffusion model. We note, however, that the model uncertainty values for R_s (provided by the Gamry circuit model output) are approximately four times bigger than the actual value for both polymers. The large uncertainty in Rs is due to limitations in potentiostat accuracy

at high frequencies, which prevented impedance measurements close to the pure series resistance range.

- **Constant Phase Element (CPE)**. CPE values given in Table 3.2 represent the admittance (inverse impedance) of electrode double layer capacitance: $1/Z_{CPE} = (j\omega)^{\alpha}Y_0$. The equivalent circuit model value of CPE is found to be larger for MPC polymer *vs.* PPY, suggesting a more significant contribution of double layer capacitance in MPC polymer electrodes compared to PPY electrodes. This result may be due to intrinsic differences between the two polymers (which would be advantageous for MPC polymer electrodes), or it may be due to differences in surface roughness between the two electrodes.

- **Warburg impedance** (W). W provides a measurement of impedance associated with diffusion of ions. MPC polymer exhibits a Warburg impedance much smaller than PPY. This may indicate that the MPC Polymer is less resistive to ion diffusion than PPY. Further controlled tests are needed to investigate ion diffusion resistances for MPC polymer vs. PPY, as Warburg impedance may be affected by electrode microstructure, which was not examined for the planar MPC polymer and PPY electrodes tested here.

- **Charge-transfer resistance** (R_{ct}). R_{ct} represents the resistance to oxidation and reduction of the electrode material. R_{ct} is about four times bigger for PPY than MPC polymer. This result may be due to greater pseudocapacitance contribution for PPY vs. MPC polymer electrodes, or it may indicate that the redox reactions are slower in PPY compared to MPC polymer (further investigation is needed).

According to Gamry´s reference website, “goodness of fit” results of 10^{-3} are considered a “good” fit (with lower goodness of fit values corresponding to better agreement between model and experimental results) [79]. A “good” fit is achieved for both PPY and MPC polymer equivalent circuit models. The data from PPY represent a better fit than the one from MPC polymer, however, both equivalent circuit models achieve comparable “goodness of fit” values to those reported in the literature [74]. We believe that, due to the big error in the series resistance, the goodness of fit is highly affected. If we were to have a better R_s fit, the goodness of fit would be much better.

As we can see, the results from the EIS and the chronoamperometry test show contradictory results. I acknowledge this difference and the reason is the qualitative nature of the CPE and W parameters comparison in this test. In order to make more concise claims from the EIS test, we would require a more controlled deposition for the samples and a study on the roughness of the material and the amount of active material among others.

Cycle Life

As described in Introduction, a key technical challenge in the pursuit of biodegradable/dissolvable supercapacitor electrode materials is finding materials that degrade easily yet are stable under repeated charge-discharge cycling. The cycle life of a supercapacitor is defined as the number of charge-and-discharge cycles until capacitance decays to less than 80% of the initial capacitance. To characterize supercapacitor material durability, cycle life tests in the literature are typically conducted using 500 to 5000 charge-discharge cycles [80]. Figure 3.9

compares the percent change in capacitance of planar PPY and MPC polymer electrodes subject to 2000 CV cycles between -0.2 V and 0.5 V at 20 mV/s scan rate. As we can see in Figure 3.9, both polymers exhibit a similar capacitance decay over 2000 cycles. Minor fluctuations in capacitance are observed for both electrodes, which is a normal behavior when performing life cycle assessments [81]. Table 3.3 compares the capacitance values (as a % of nominal capacitance) for the two electrodes at 500 cycle intervals. Cycle 100 was chosen as the "nominal capacitance" to enable the electrodes to stabilize fully in the electrolyte [82]. After 2000 cycles, the capacitance of the PPY electrode has decreased by 20%, compared to a 30% decrease for the MPC polymer electrode. These results are aligned with literature values for PPY electrodes, which typically show declines of 10-35% after 1000 cycles [74], [75]. While it was expected that MPC polymer would have greater capacitance loss with repeated cycling than PPY, the results in Figure 3.9 are highly encouraging for the feasibility of MPC polymer supercapacitor electrodes. Capacitance loss in CP electrodes is caused in part by repeated stresses due to volume change of the polymer during oxidation and reduction (volume changes as high as 35% have been reported [83]). Cycle life of CP supercapacitor electrodes can be extended by depositing the CP on a flexible nanomaterial substrate, such as carbon nanotubes.

Dissolution Testing

To test the solubility of MPC polymer in mild aqueous conditions, planar PPY and MPC electrodes were immersed in a 37 ^{o}C heated bath at a pH of 8.2

(Figure 3.10). Tris acetate-EDTA buffer solution was used to control the pH at 8.2. According to Zelikin *et al.*, these "mild aqueous conditions" are sufficient to dissolve a PPY derivate similar to MPC polymer in a period of 24 hours [70].

Figure 3.11 compares photographs of the MPC polymer (3.11a) and PPY (3.11b) electrodes at hourly intervals during dissolution testing. After 4 hours, the MPC polymer coating has dissolved while the PPY coating is intact (no visible change). Figure 3.12 compares photographs of the MPC polymer electrode before and after dissolution testing (with the sample out of solution). A brown residue can be seen on the electrode surface of the MPC polymer sample after 4 hours. This thin residue layer is most likely due to the covalent Au-MPC polymer bond, which is expected to be stronger than van der Waals crosslinking of MPC polymer chains. This residue did not dissolve or change visibly after many more hours in the heated bath.

Summary and Future Work

At the beginning of this chapter, we introduced the need to find an electrode material that dissolves in mild aqueous conditions and has supercapacitor performance characteristics competitive with state-of-the-art electrode materials. Following the work of Zelikin *et al.* approach to erodible CPs, the MPC polymer was chosen as a derivative of the widely-used conductive polymer PPY. Both share the same main chain while the MPC polymer features methyl carboxylate side structures that promote dissolution under mild conditions. CV, chronoamperometry, EIS, and cycle life measurements were performed comparing PPY and MPC polymer planar electrodes. The performance of the MPC polymer electrode was

found to be comparable to that of state-of-the-art PPY, suggesting that the MPC polymer is a viable CP for electrochemical energy storage applications. The ease of dissolution of the MPC polymer electrode was also confirmed.

As described in the Introduction, supercapacitor charge storage is enhanced through the use of high surface area, porous electrode materials. This chapter utilized a planar, Au-coated substrate for preliminary testing of the MPC polymer as a supercapacitor material. The next step in this work is to find a substrate that is porous, soluble, and nontoxic that can suit the proposed applications of the MPC polymer. In the following section, we propose a nanocellulose-based MPC polymer supercapacitor electrode that combines the desirable pseudocapacitive and erodible properties of MPC polymer with the high surface area, porous characteristics of nanocellulose.

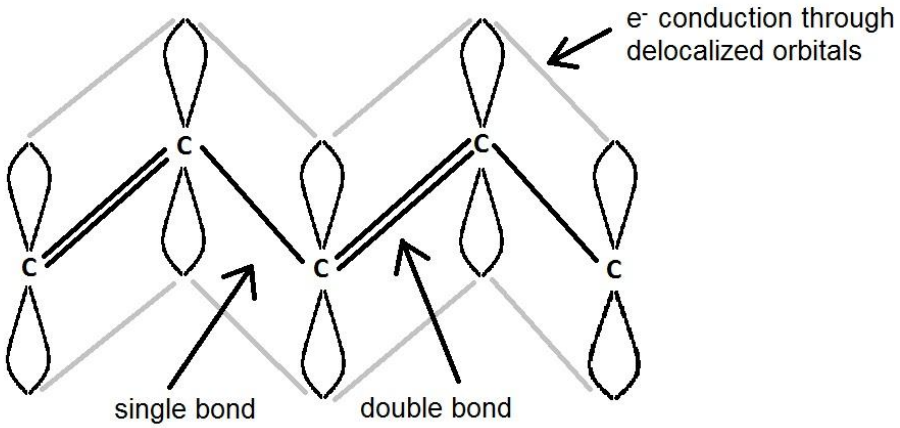

Figure 3.1 CP conduction mechanism. Illustrated for polyacetylene, a CP that presents the simplest conjugated backbone. Delocalized orbitals and the conduction of electrons through the pi-conjugation are shown.

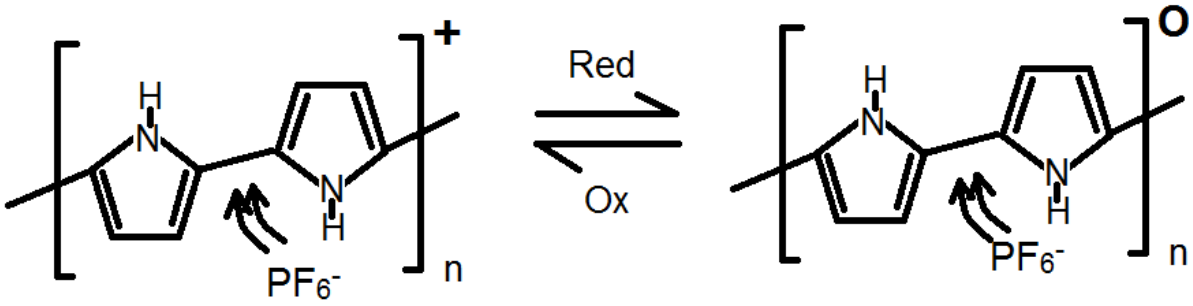

Figure 3.2 Pseudocapacitance mechanism of PPY. Oxidation representation.

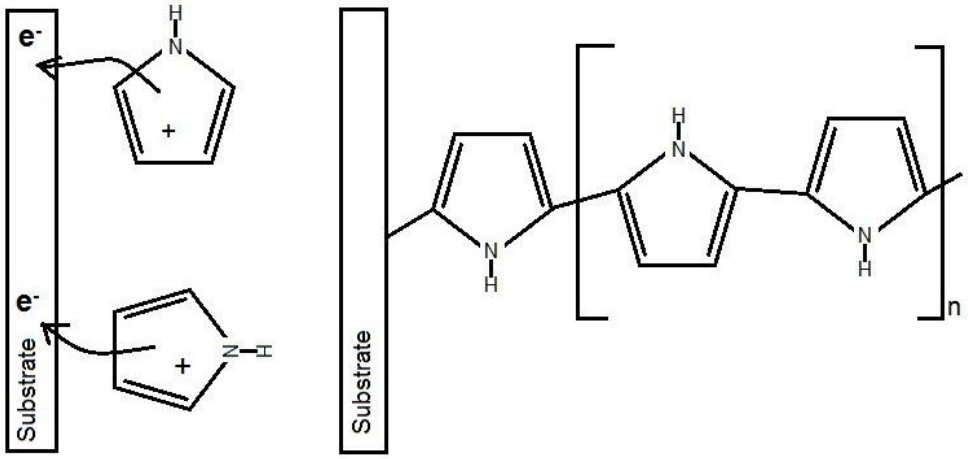

Figure 3.3 Electrodeposition mechanism for PPY.Pyrrole monomers in contact with the deposition substrate are electrochemically oxidized leading to polymer chain formation and doping with electrolyte ions [72].

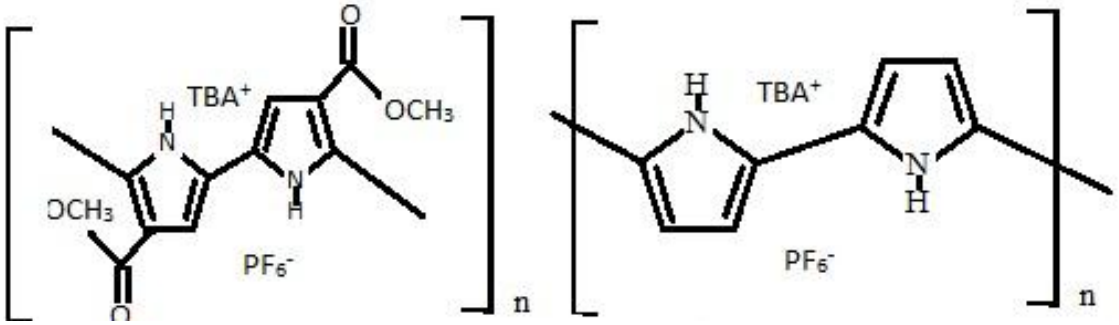

Figure 3.4 Polymers structural comparison: MPC polymer (left) and PPY (right), both with $TBAPF_6$ dopant.

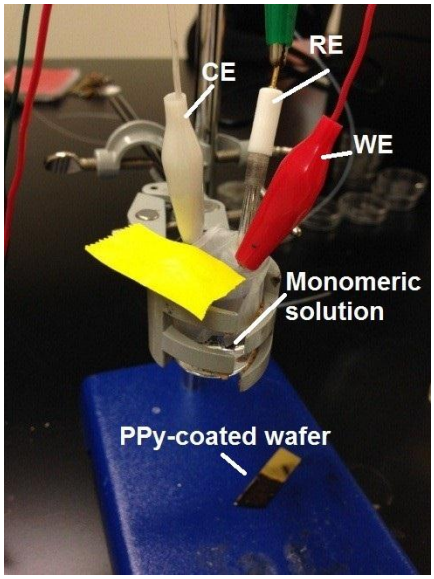

Figure 3.5 Polymer electrodeposition. Set-up with Pt wire counter electrode (CE), Ag/Ag+ reference electrode (RE) and a Au-coated Si wafer as the deposition substrate (working electrode, WE).

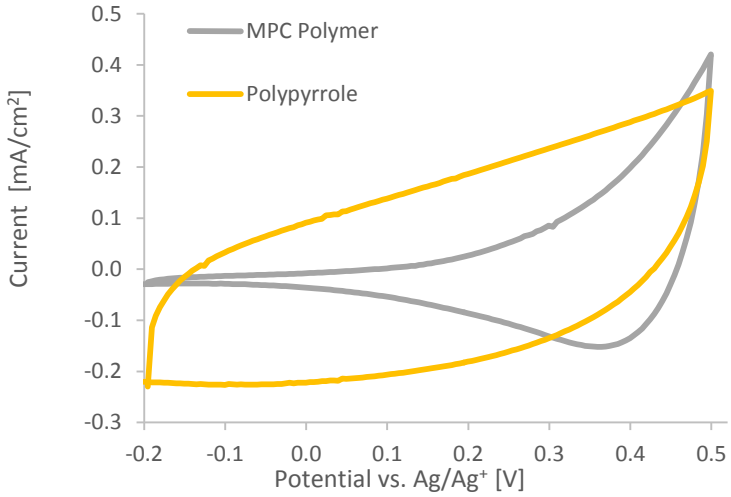

Figure 3.6 CV measurement. Ag/Ag+ reference electrode for MPC polymer and PPY.

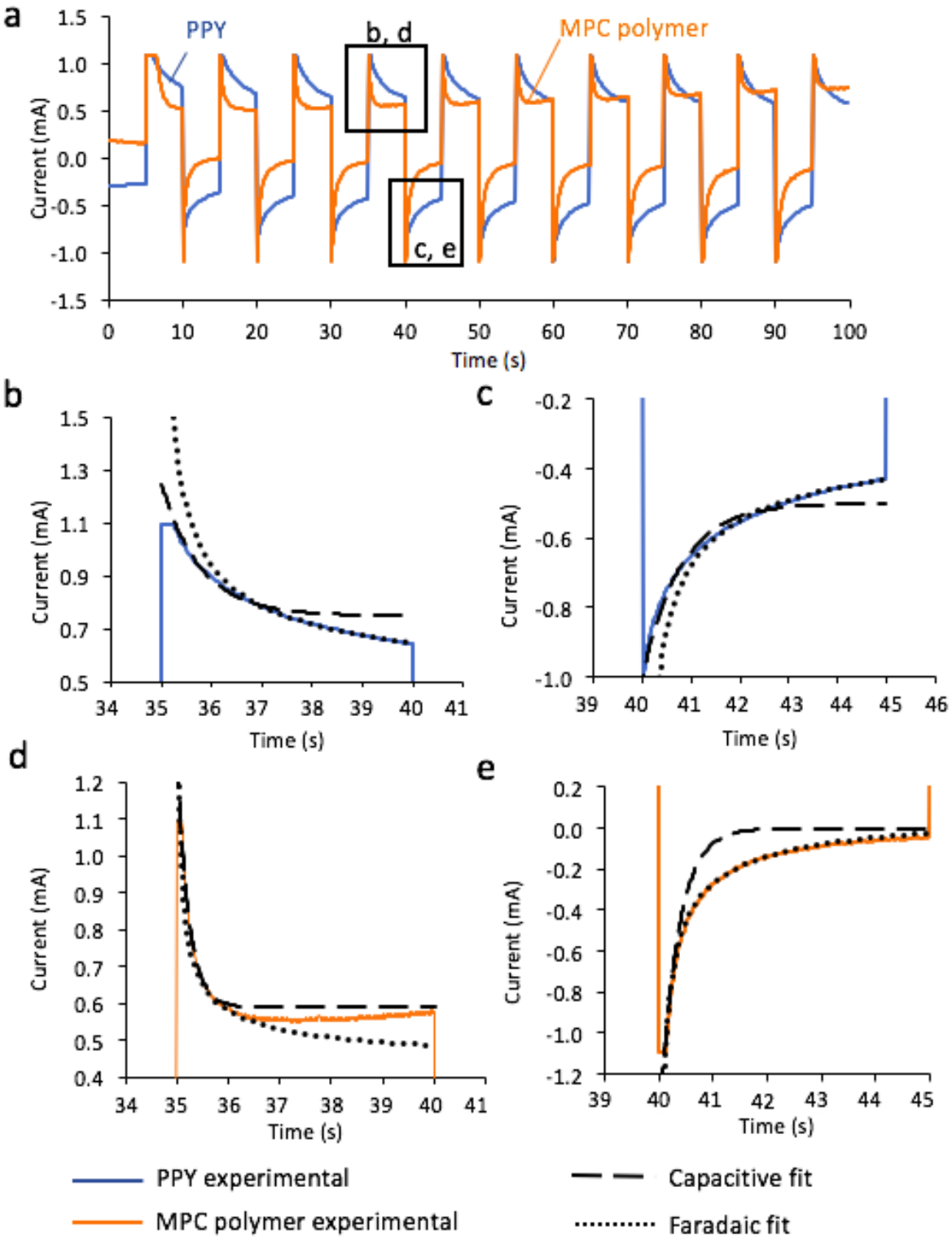

Figure 3.7 Chronoamperometry results and current model fits for PPY and MPC polymeric. Experimental current for 10 charge-discharge cycles. Capacitive and faradic current models for: b) PPY anodic current, c) PPY cathodic current, (d) MPC polymer anodic current, and (e) MPC polymer cathodic current profiles.

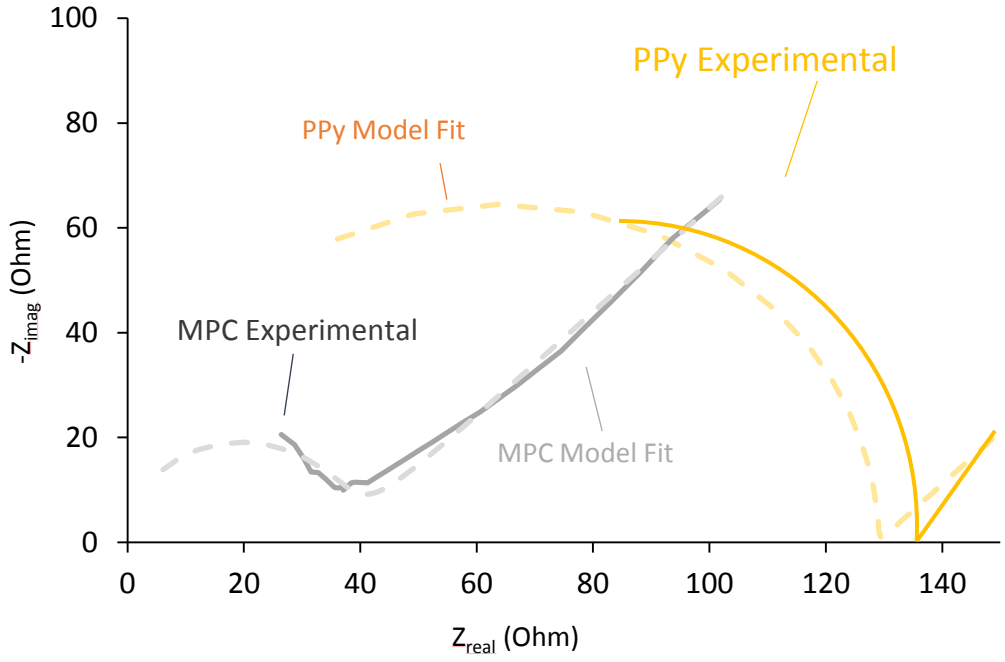

Figure 3.8 EIS presented in a Nyquist plot for MPC polymer and PPY. Experimental results are given as solid lines, and CPE model fits as dashed lines.

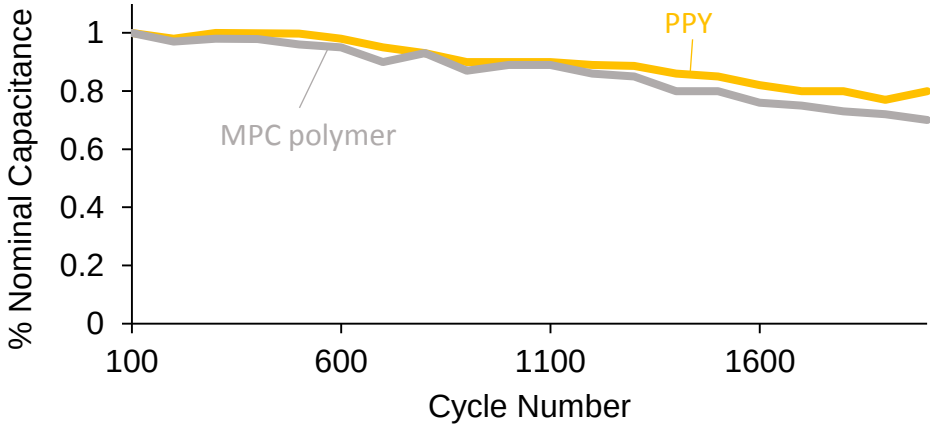

Figure 3.9 Life assessment graph. Comparison of capacitance change in PPY and MPC polymer electrodes over 2000 CV cycles.

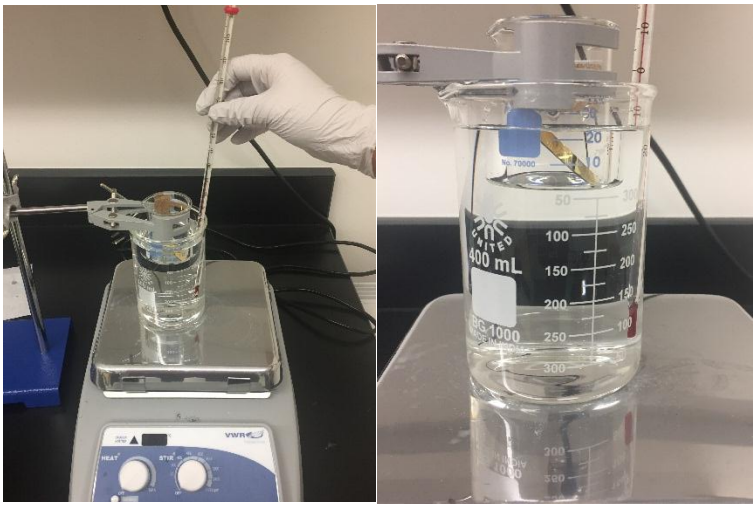

Figure 3.10 Warm bath and dissolution test set-up.

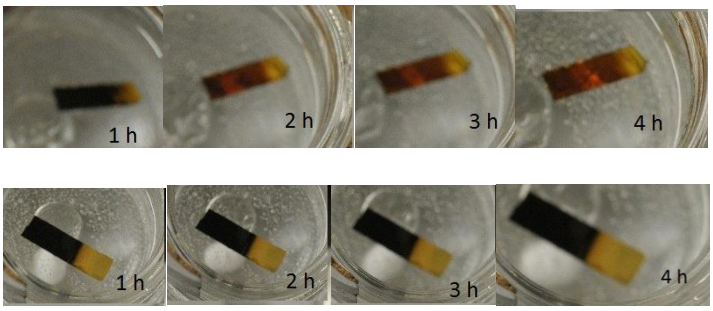

Figure 3.11 MPC polymer and PPY dissolution images. a) MPC polymer in mild aqueous conditions for 4 hours. b) PPY in mid aqueous conditions for 4 hours

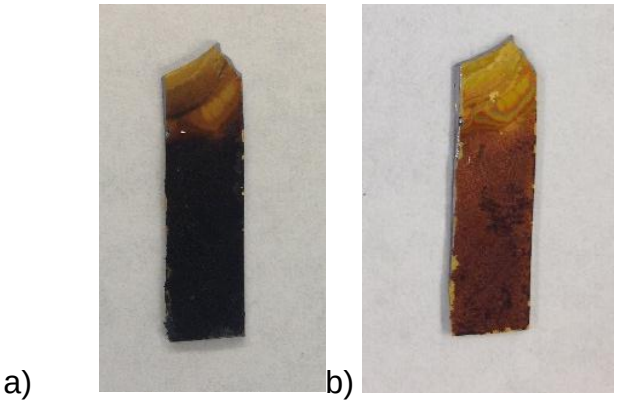

Figure 3.12 MPC polymer electrodes. a) Before dissolution test. b) After 4 hours in 8.2 pH solution at 37 º C.

Table 3.1 Equations for the capacitive and faradic fit for PPY and MPC polymer charge-discharge current profiles.

Electrode	***Capacitive Fit***	***Faradic Fit***
PPY (anodic current)	$I_{cap} = 0.5e^{-1.3t} + 0.75$	$I_{far} = 0.53t^{-0.5} + 0.41$
PPY (cathodic current)	$I_{cap} = -0.5e^{-1.3t} - 0.5$	$I_{far} = -0.45t^{-0.5} - 0.23$
MPC polymer (anodic current)	$I_{cap} = 0.7e^{-4.5t} + 0.59$	$I_{far} = 0.17t^{-0.5} + 0.41$
MPC polymer (cathodic current)	$I_{cap} = -1.5e^{-3t}$	$I_{far} = -0.45t^{-0.5} + 0.18$

Table 3.2 CPE with diffusion model fit for PPY and MPC polymer.

Parameter	*PPy*	*MPC Polymer*	*Units*
Rs	2.49 ± 11	1.33 ± 9	Ohms
CPE	2 ± 1	27 ± 1	10^{-9} S*s^{-a}
W	11 ± 1	0.5 ± 1	10^{-3} S*$s^{1/2}$
Rct	129 ± 3	36 ± 6	Ohms
Goodness of fit	8.213 e-3	36.68 e-3	

Table 3.3 Selected points from PPY and MPC polymer life assessment.

CYCLE NUMBER	% INITIAL CAPACITANCE MPC POLYMER	% INITIAL CAPACITANCE PPY
100	100	100
500	97	99
1000	90	90
1500	80	83
2000	70	80

MPC POLYMER ON A NANOCELLULOSE SUBSTRATE

The previous section introduced the MPC polymer as a supercapacitor electrode material that has comparable supercapacitor performance to state-of-the-art PPY and dissolves in mild aqueous conditions. This is a significant contribution to the field of transient electronics and enables new applications for electrochemical energy storage where solubility or erodibility is required. In this section, we introduce the deposition of the MPC polymer on a nanocellulose high surface area soluble substrate and analyze the electrode's supercapacitor performance and solubility.

Nanocellulose as a Porous Substrate

There are many different types of substrates that are porous and can provide high surface area. Especially now that supercapacitors are a growing technology, many different materials are engineered in order to achieve the best performance possible; graphene and carbon nanotubes are good examples. However, those substrates present different disadvantages from toxicity to environmental unfriendliness and medical incompatibility. Carbon nanotubes ("CNTs"), for example, are not intrinsically dissolvable nor biodegradable [84], [85]. Some researchers have published ways to make them soluble and biodegradable, and many publications address this and the toxicity associated with doing so [86]–[88]. The toxicity levels of CNTs for different applications have been studied by

different research groups. Many researchers conclude that CNTs are dangerous for medical and implantable uses, including when modified to be dissolved or degraded [89]–[91]. In addition, CNTs are expensive and resource-consuming to massively synthesize [92].

Cellulose is a sustainable alternative that can be used as a high surface area, porous substrate. Cellulose is the main constituent of plant cell walls and vegetable fibers: it is a sustainable material coming from a sustainable source. Cellulose is at the same time low cost, nontoxic, biocompatible and easy to obtain [93]–[95]. There are many different forms of cellulose with different properties. Among those are paper and nanocellulose, both of which have been demonstrated in the electronics and electrochemical energy storage fields. Paper, in particular, can be combined with a functional material to produce not only supercapacitors but also diodes, transistors, electric circuits, etc. [96]. In 2016, Cagang *et al.* published a graphene-based field effect transistor using a two-dimensional ("2D") paper network [97]. Zheng *et al.* released in 2013 a demonstration on desktop printed electronics [98]. Xioliang Zeng *et al.*, published a flexible dielectric for energy storage based on CNT and cellulose [99]. Nanocellulose is used for a wide range of purposes like printed electronics, electronics, composites, medical supplies and implants, energy sensors, energy harvesting, and microfluidics [95]–[97] Cherian *et al.* reported using nanocellulose for medical implants in 2013 [103]. Lu *et al.* used nanocellulose to modify polymer composites in order to achieve different properties for medical materials [104]. Additionally, Tian *et al.* reported using nanocellulose in order to create a Raman scattering substrate [105].

For supercapacitor applications, nanocellulose-based electrodes have been demonstrated that achieve performance metrics similar to those obtained with CNTs, with all the advantages from cellulose [106]–[108]. Nanocellulose particle sizes range from 3 to 100 nm. Their nanometric size makes them a very attractive material for supercapacitors, from producing porous aerogels, to assisting the gelation of graphene oxide aerogels, to direct use as porous substrates for supercapacitors [109]–[111]. Previous work has demonstrated nanocellulose combined with CPs (polyaniline and PPY) for supercapacitor electrodes [107], [108]. Surface modification of nanocellulose can be used to improve the chemical and mechanical stability of cellulose, as described by Zoppe *et al.* [112]. Wang *et al.* used surface-modified cellulose to enhance the capacitance of their supercapacitor design based on conductive polymers [106]. In this work, unmodified nanocellulose is used to simplify the synthesis procedure; future work could investigate potential benefits of surface modification for CP-nanocellulose supercapacitor performance.

In this chapter, nanocellulose is used as a substrate for the MPC polymer with the purpose of achieving a high-surface area, fully-dissolvable supercapacitor. In order to optimize the surface area, we are chemically depositing the MPC polymer onto the nanocellulose particles and then binding them together as described in the Experimental section. This is the first use of the MPC polymer on a dissolvable substrate with demonstrated dissolution.

Experimental

High purity microcrystalline cellulose (nanocellulose) was purchased from Chem Center @ Amazon.com. The rest of the chemicals involved in the chemical deposition of the MPC polymer were purchased from Sigma-Aldrich. All materials were used as received.

MPC polymer-nanocellulose composites were prepared after the method described by Tammela *et al.* to chemically deposit PPY on algae-based cellulose [106]. Significant alterations were made to the procedure of Tammela *et al.*, including using acetonitrile instead of water to allow MPC to mix with the rest of the chemicals, adding 3 times (“x”) the amount of nanocellulose than the paper explains, and sonicating the beaker all throughout the deposition to prevent nanocellulose agglomeration prior to MPC polymer coating.

Nanocellulose (600 mg) is first added to 10 mL acetonitrile and sonicated for about 5 min while the next solution is prepared. In a separate solution, methyl 1H-pyrrole-3-carboxylate (MPC) monomer (0.2 g) is mixed with 2-3 drops of Tween 80 in 10 mL acetonitrile and stirred for 5 min at 250 rpm. Tween 80 is a surfactant that assists with the dissolution of MPC monomer in nanocellulose. This solution is then added to the nanocellulose and sonicated for as long as we need to prepare the next solution. The oxidizing agent is prepared by adding 2 gm $FeCl_3$ to 15 mL acetonitrile with gentle stirring. The oxidizing solution is then added to the prepared nanocellulose-MPC monomer solution. The final solution is sonicated for 1 to 2 h and left overnight to produce a thick black slurry. The slurry is placed on a filter and rinsed several times with acetonitrile to remove the residual $FeCl_3$. Following

the rinse step, the MPC polymer-nanocellulose slurry is mixed in an alcohol solution with 1 % wt. PTFE binder to help it attach to the Au-coated Si electrode for electrochemical testing.

Supercapacitor Electrode Performance

CV, chronoamperometry, and EIS measurements were conducted to characterize the supercapacitor performance of MPC polymer-nanocellulose composite electrodes. The results are compared with the previous chapter results for planar MPC polymer electrodes to assess the performance improvement with the nanocellulose composite. Experimental parameters and the three-electrode cell setup are the same as described previously.

Cyclic Voltammetric

Figure 4.1 compares CV measurements for pure nanocellulose and MPC polymer-nanocellulose composite electrodes. CV measurements were conducted with a potential range between -0.2 and 0.5 V vs. Ag/Ag+ at a scan rate of 100 mV/s. This potential range was selected following the CV parameters used in the previous section. A specific capacitance of 47 F/g for the MPC polymer-nanocellulose composite is obtained from the measurements in Figure 4.1 using Equation 2.2. CV measurements of the pure Au-coated Si substrate are also included in Figure 4.1 to isolate the capacitive contributions of the nanocellulose vs. the electrode substrate. As we can see, the capacitance of the wafer alone and the nanocellulose-coated wafer are negligible compared to the MPC-coated wafer. The specific capacitance of the pure nanocellulose electrode was calculated as

1.54 F/g, indicating a 306% increase in capacitance with addition of the MPC polymer.

The specific capacitance measured here for MPC polymer-nanocellulose composite is low compared to values reported for PPY-nanocellulose (e.g., Wang *et al.* obtained capacitances of 140-180 F/g for PPY-nanocellulose electrodes [106]). This could be due in part to the lower faradaic capacitance of MPC polymer compared to PPY, as reported in the previous chapter. Further improvements to the specific capacitance of the MPC polymer-nanocellulose electrode could be achieved by increasing the weight ratio of MPC polymer to nanocellulose and/or testing different oxidation procedures to obtain the best method of MPC polymer-nanocellulose electrode preparation. It is also observed that the shape of the MPC polymer-nanocellulose curve in Figure 4.1 differs significantly from that of the planar MPC polymer electrode reported in the previous section (Figure 3.6). This is expected given the significant difference in substrates (planar Au vs. nanocellulose), as CV profiles are determined in part by ion diffusion rates and electrical properties of the substrate [113]. Another possibility is that the anodic current peak is due to residual $FeCl_3$ left over from the chemical deposition of MPC polymer (the reduction potential of Fe^{3+} in acetonitrile is approximately 0.2 V vs. Ag/Ag+).

Chronoamperometry

Chronoamperometry measurements for the MPC polymer-nanocellulose electrode were conducted by applying alternating step potentials of 0 V and 0.5 V

(5 s at each potential) (same test conditions as in the previous section). Figure 4.2a shows charge-discharge current measurements for the MPC polymer-nanocellulose electrode; Figure 4.2b and 4.2 present capacitive and faradic models of anodic and cathodic currents, respectively. Table 4.1 shows the equations used for capacitive and faradic fits of the experimental current data.

As we can see in Figures 4.2b and 4.2c, the faradic fit represents accurately the behavior of the MPC polymer-nanocellulose electrode (with the capacitive current model providing a good fit for the first milliseconds of charging or discharging). Asymmetries in cathodic and anodic current profiles noted in the previous section for planar MPC polymer electrodes are not observed for the nanocellulose-based electrode. This suggests that the anodic current irreversibilities of planar MPC polymer electrodes are not intrinsic to the MPC polymer (a promising result for achieving a long cycle life electrode material).

Electrochemical Impedance Spectroscopy

Figure 4.3 compares EIS results for the MPC polymer-nanocellulose electrode presented in this chapter with planar MPC polymer electrode results from the previous section. For the MPC polymer-nanocellulose electrode, it was not possible to obtain a good equivalent circuit model fit of the results because of large measurement errors at high frequencies. The following observations can be made by comparing the Nyquist curves for MPC polymer-nanocellulose and planar MPC polymer electrodes:

- **Series resistance**. Extrapolating the Nyquist curve for MPC polymer-nanocellulose, we estimate an R_S value of $< 5\ \Omega$. This value is comparable

to that obtained for MPC polymer on Au (1.3 Ω, Table 3.2), suggesting that the MPC polymer is well-coated on the nanocellulose. It also indicates that the 1% nonconductive PTFE binder added to the MPC polymer-nanocellulose electrode is not significantly impacting the overall electrode conductivity.

- **Charge-transfer resistance**. EIS results in Figure 4.3 indicate that the cellulose-based electrode has higher R_{ct} compared to planar MPC polymer. R_{ct} is a complex reaction kinetics parameter that is known to depend on the materials present in the electrochemical system. The increase in R_{ct} observed for MPC polymer-nanocellulose electrode could be due to residual Fe_3Cl. Further investigation is needed to determine the role of nanocellulose in increasing R_{ct} for MPC polymer electrodes.

Dissolution Testing

Following electrochemical testing, we assessed the dissolution ability of the MPC polymer-nanocellulose composite electrode in mild aqueous conditions. The electrode was placed in an aqueous solution of tris acetate buffer (pH 8.2) at ambient temperature. The solution was stirred slowly at 60 rpm to promote diffusion of the liquid in between the cellulose particles. The objective of this test set-up was to ensure that the nanocellulose particles would break-up easily in solution, enabling the MPC polymer coating to subsequently dissolved (as proved in the previous section). Stirring was used to disperse the nanocellulose particles once they have broken apart since, due to their weight, they stayed sitting on top of the wafer. Elevated temperature was not necessary to break apart the nanocellulose substrate. Figure 4.4a provides a picture of the as-prepared MPC

polymer-nanocellulose electrode; Figure 4.4b illustrates the electrode dissolution with slow stirring. After 30 min, the electrode has broken apart and a powder is left in the solution.

Summary and Future Work

At the beginning of this chapter, we posed the question “Can we design a dissolvable electrode with a porous substrate?” In this design, we utilize a nanocellulose porous substrate and the previously characterized MPC polymer as the active material. Nanocellulose was selected as nontoxic, cheap, lightweight, dissolvable, and highly-porous substrate for MPC polymer supercapacitor electrodes. CV, chronoamperometry, and EIS measurements indicate that MPC polymer-nanocellulose electrodes have good capacitance, faradic charge-storage characteristics, and low equivalent series resistance. In addition, cathodic current irreversibilities observed in the third chapter for planar MPC polymer electrodes were eliminated for MPC polymer-nanocellulose composite electrode. The nanocellulose substrate breaks apart easily in mild aqueous conditions, and is therefore a good choice of porous electrode substrate for the MPC polymer. The results presented in this section affirm MPC polymer-nanocellulose composite as a promising supercapacitor electrode material. Further research is needed to optimize the composite synthesis process to improve specific capacitance. Further investigation should also include material characterization like scanning electron microscopy

(SEM) imaging to determine the microstructure of the composite electrodes, and more in-depth study of the effect of relative volumes, thicknesses and masses

of both active materials on the performance of the MPC polymer-nanocellulose electrodes.

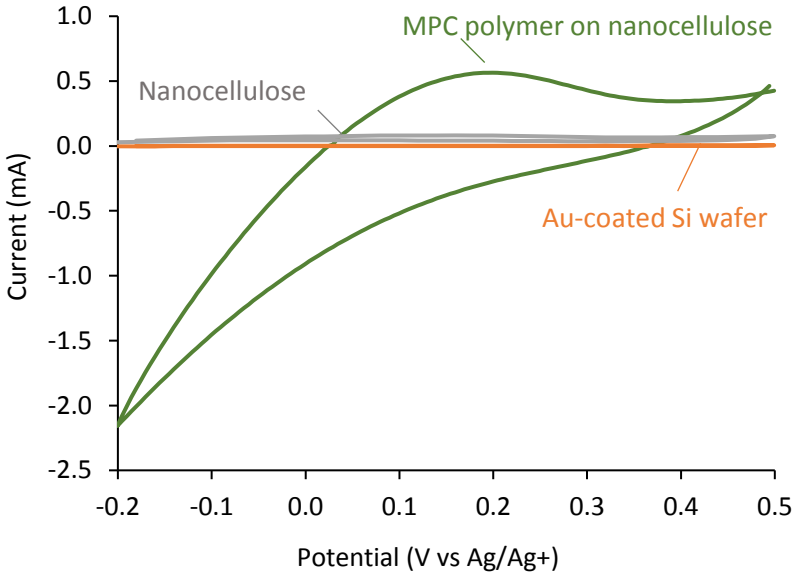

Figure 4.1 CV measurement for MPC polymer on nanocellulose substrate. Overlapped CV measurements for MPC polymer on nanocellulose on Au-coated silicon wafer, nanocellulose on Au-coated Si wafer, and Au-coated Si wafer alone.

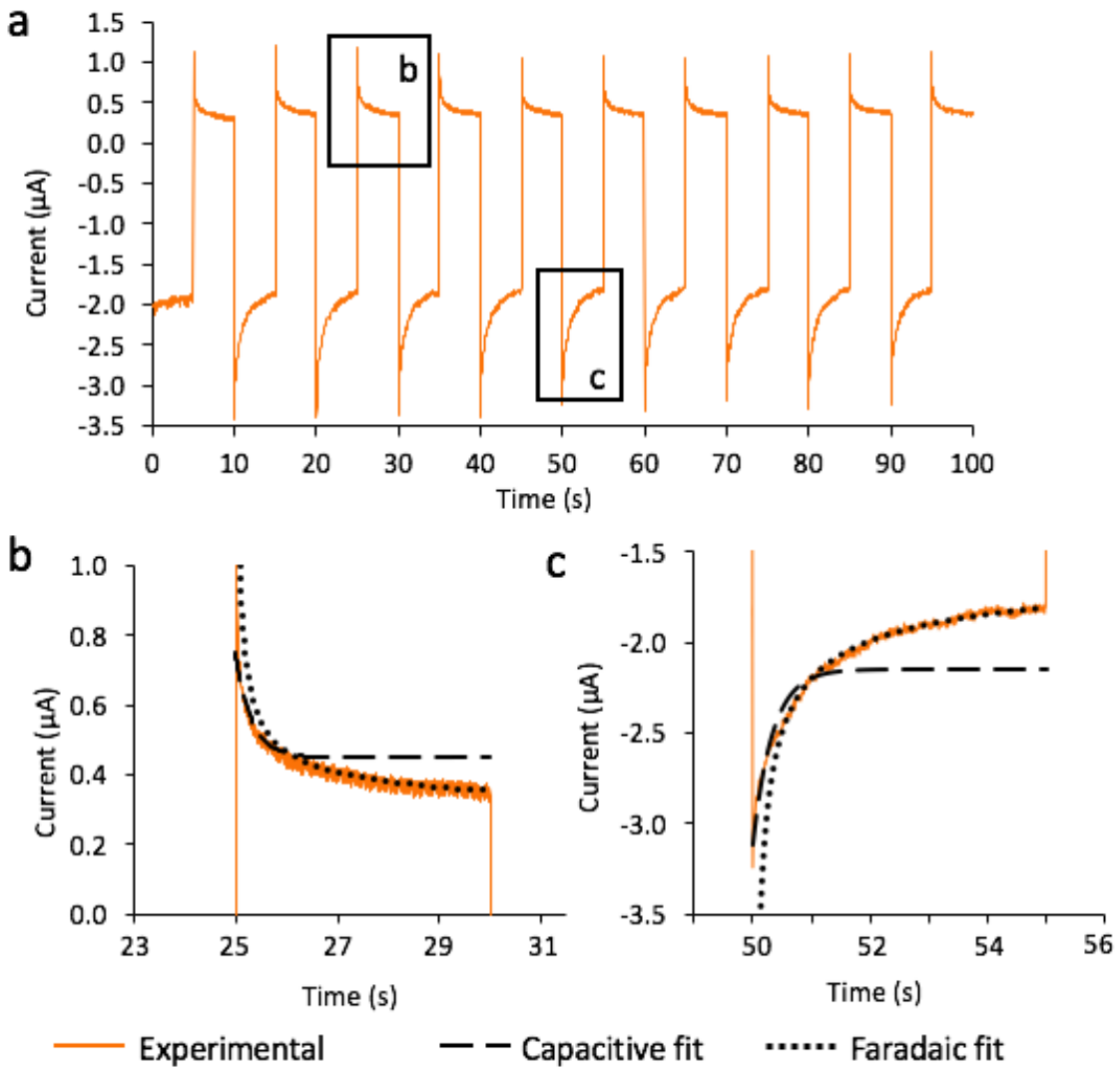

Figure 4.2 Chronoamperometry for MPC polymer on nanocellulose substrate. a) Charge-and-discharge measurement for 10 cycles on MPC polymer-coated nanocellulose. Capacitive and faradic current model fit for: b) charging (cathodic) current, and c) discharging (anodic) current).

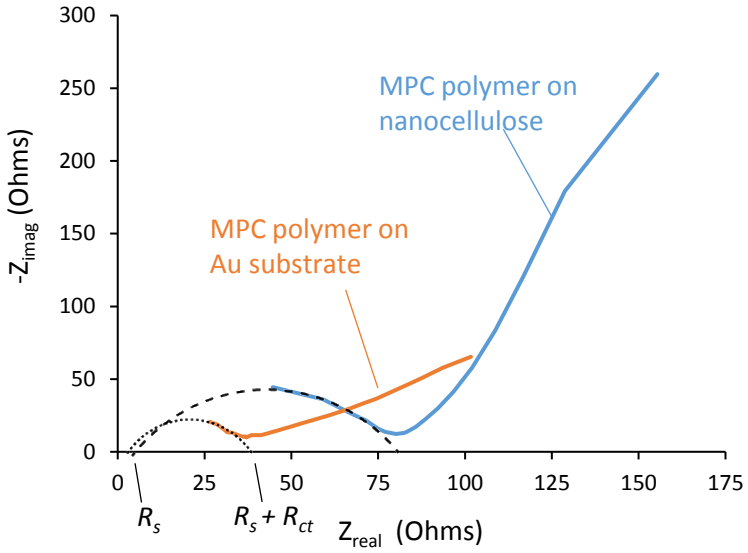

Figure 4.3 Comparison of EIS results for MPC polymer-nanocellulose and planar PC polymer electrodes, presented as a Nyquist plot. Dotted and dashed semicircles show approximate values of series and charge-transfer resistances for planar MPC polymer and MPC polymer-nanocellulose electrodes, respectively.

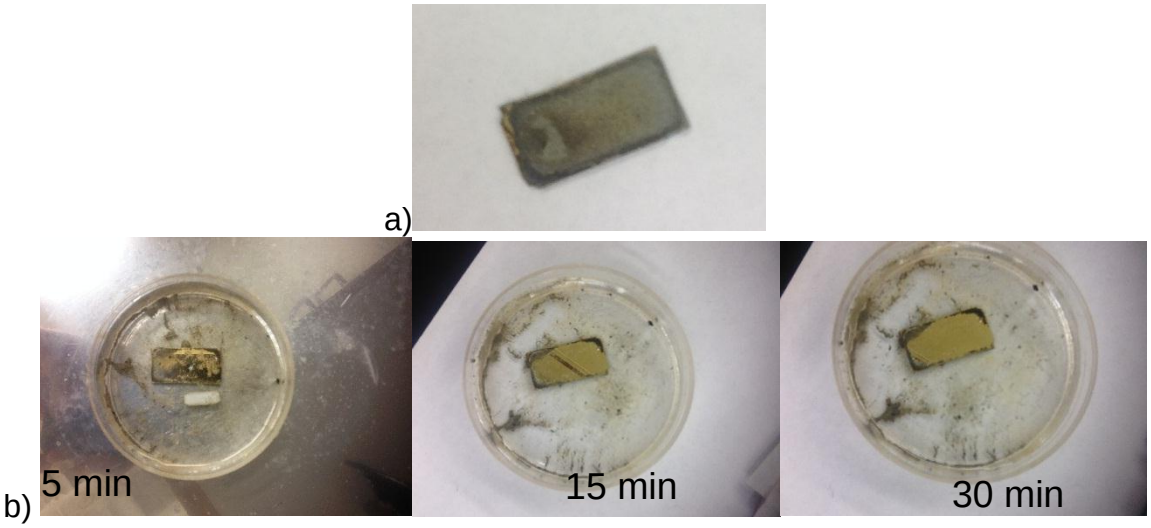

Figure 4.4 MPC polymer on nanocellulose dissolution test.a) Electrode before dissolution test. b) Dissolution images at 5, 15, and 30 min.

Table 4.1 Parameters used to achieve the best fit for capacitive and faradic behavior of MPC polymer-nanocellulose electrodes.

	Capacitive Fit Equation	*Faradic Fit Equation*
Anodic current	$I_{cap} =$ $(4\text{x}10^{-8}\ e^{-3.2t}+0.45)$	$I_{far} = 0.2t^{-0.5} + 0.265$
Cathodic current	$I_{cap} = -1e^{-3t} - 2.15$	$I_{far} = -0.7t^{-0.5} - 1.5$

SUMMARY, CONCLUSIONS, AND FUTURE WORK

At the beginning of this thesis, we posed the research question: can we find a conductive polymer that dissolves in mild aqueous conditions and achieves supercapacitor performance metrics comparable with nonbiodegradable, state-of-the-art conductive polymers? To approach this challenge, we followed Zelikin's [70] approach to erodible conductive polymers. The MPC polymer studied in this work has a main chain structure identical to PPY, and features side methyl carboxylate side-chain groups to promote solubility.

The previous section investigated the electrodeposition of MPC polymer onto a Au-coated Si wafer and characterized the material through CV, chronoamperometry, EIS, and cycle life measurements. We found that the MPC polymer has a capacitance similar to state-of-the-art PPY. Through chronoamperometry measurements we observed that MPC polymer utilizes a faradic (redox) charge storage mechanism, confirming its operation as a pseudocapacitive material similar to PPY. EIS measurements and equivalent circuit modeling indicate lower equivalent series resistance, charge transfer resistance, and Warburg impedance for MPC polymer electrodes compared to PPY. This result is promising for achieving high power density supercapacitor electrodes with MPC polymer, as supercapacitor power is inversely proportional to electrode resistance. Cycle life measurements indicate that both MPC polymer and

PPY electrodes follow a similar trend in capacitance loss over 2,000 charge-discharge cycles (30% capacitance loss for MPC polymer, vs. 20% for PPY). At the end of the previous section, we proved the dissolution of the MPC polymer in mild aqueous conditions. Having demonstrated that the MPC polymer achieves comparable supercapacitor performance as state-of-the-art CPs and is dissolvable, we moved on to finding a high surface area, biocompatible substrate material for MPC polymer electrodes.

Nanocellulose was selected as a low-cost, environmentally-friendly electrode material that is well-studied for biomedical applications and transient electronics. We deposited the MPC polymer chemically, instead of electrochemically, on the nanocellulose substrate to obtain a composite electrode (electrochemical deposition is limited to conductive substrates). The MPC polymer-nanocellulose composite has a capacitance of 47 F/g, a 1.54 F/g capacitance increase compared to pure nanocellulose (as determined by CV measurements). Additionally, irreversibilities observed in the discharge mechanism of planar MPC polymer were eliminated with the MPC polymer-nanocellulose electrode, which follows a pure faradic current model. The EIS comparison between the planar substrate and the nanocellulose substrate indicated only a slight increase in equivalent series resistance for the nanocellulose electrode. Finally, we proved the dissolution of the MPC polymer-nanocellulose electrode by observing the easy breaking apart of the nanocellulose composite upon gentle stirring.

We can now state that we have found a conducting polymer that dissolves

in mild aqueous conditions and works as an energy storage active material. This is the first step in developing dissolvable supercapacitors for biomedical applications, transient electronics, as well as environmental applications. This work is to the best of our knowledge the first demonstration of the MPC polymer being used for electrochemical energy storage and the first demonstration of a conductive polymer used for electrochemical energy storage that dissolves in mild aqueous conditions.

After this study and its positive results, there are many possible directions to propose for future work. First, it is necessary to perform a toxicity study on the MPC polymer to assess its viability as an energy storage material for environmental sensors. Second, we would like to perform a biocompatibility study to assess possible applications of the MPC polymer in implantable devices and medical applications. Previous work has proposed integrating PPY in small quantities in implantable devices; we are therefore optimistic that the MPC polymer may have promising biomedical applications as it would have less likelihood of accumulating in the body [70]. Further study is needed to test this hypothesis.

Finally, further work is needed to optimize the supercapacitor performance of dissolvable CP electrodes through testing different synthesis procedures and materials. This work did not perform an optimization of the chemical deposition or postprocessing of the electrode material; better energy storage performance can be expected were these to be performed. The next steps in this research line could also include trying different polymers with the same methyl carboxylate side groups, or trying the same main chain with different side groups. Further research

is also needed to test other high surface area, bio-friendly substrates (such as poly-L-lactic acid scaffolds) that can lead to enhanced performance of MPC polymer supercapacitor electrodes.

REFERENCES

[1] S. Chu and A. Majumdar, “Opportunities and challenges for a sustainable energy future,” *Nature*, vol. 488, no. 7411, pp. 294–303, Aug. 2012.

[2] D. Lindley, “The energy,” *Nature*, vol. 463, pp. 18–20, 2010.

[3] S. Badwal, S. S. Giddey, C. Munnings, A. I. Bhatt, and A. F. Hollenkamp, “Emerging electrochemical energy conversion and storage technologies,” *Front. Chem.*, vol. 2, pp. 1–28, 2014.

[4] E. S. Beh, D. De Porcellinis, R. L. Gracia, K. T. Xia, R. G. Gordon, and M. J. Aziz, “A neutral pH aqueous organic − organometallic redox flow battery with extremely high capacity retention,” *Energy Lett.*, vol. 2, pp. 639–644, 2017.

[5] J. Fu, Z. P. Cano, M. G. Park, A. Yu, M. Fowler, and Z. Chen, “Electrically rechargeable zinc – air batteries : progress , challenges , and perspectives,” *Adv. Mater.*, vol. 1604685, 2017.

[6] D. Sheberla, J. C. Bachman, J. S. Elias, C. Sun, and Y. Shao-horn, “Conductive MOF electrodes for stable supercapacitors with high areal capacitance,” *Nat. Mater.*, vol. 16, pp. 220–224, 2017.

[7] X. Chen *et al.*, “Electrochromic fiber-shaped supercapacitors,” *Adv. Mater.*, vol. 26, no. 48, pp. 8126–8132, 2014.

[8] J. C. Ellenbogen, “Supercapacitors: a brief overview,” *MITRE*, pp. 1–34, 2006.

[9] J. Moreno, M. E. Ortúzar, J. W. Dixon, and S. Member, “Energy-management system for a hybrid electric vehicle , using ultracapacitors and neural networks,” *IEEE Trans. Ind. Informatics*, vol. 53, no. 2, pp. 614–623, 2006.

[10] M. A. Guerrero, E. Romero, F. Barrero, and P. Electronics, “Supercapacitors : alternative energy storage systems,” *ResearchGate*, vol. 3, 2009.

[11] F. Wu, C. Rüdiger, and M. R. Yuce, “Real-time performance of a self-powered environmental IoT sensor network system,” *MDPI*, pp. 1–14, 2017.

[12] A. Pandey, F. Allos, A. P. Hu, and D. Budgett, “Integration of supercapacitors into wirelessly charged biomedical sensors,” *IEEE Trans. Ind. Informatics*, pp. 56–61, 2011.

[13] J. Maeng, C. Meng, and P. P. Irazoqui, “Wafer-scale integrated micro-supercapacitors on an ultrathin and highly flexible biomedical platform,” *NCBI*,

2015.

[14] M. Conte, “Supercapacitors technical requirements for new applications,” *Fuel Cells*, vol. 10, no. 5, pp. 806–818, 2010.

[15] J. Vatamanu and D. Bedrov, “Capacitive energy storage: current and future challenges,” *ACS Publ.*, vol. 6, no. 18, pp. 3594–3609, 2015.

[16] G. Z. Chen, “Progress in natural science : materials international understanding supercapacitors based on nano-hybrid materials with interfacial conjugation,” *Prog. Nat. Sci. Mater. Int.*, vol. 23, no. 3, pp. 245–255, 2013.

[17] A. Yu, Z. Chen, R. Maric, L. Zhang, J. Zhang, and J. Yan, “Electrochemical supercapacitors for energy storage and delivery: advanced materials , tachnologies and applications,” *Appl. Energy*, vol. 153, pp. 1–2, 2015.

[18] H. Ji *et al.*, “Capacitance of carbon-based electrical double-layer capacitors,” *Nat. Commun.*, vol. 5, pp. 1–7, 2014.

[19] M I T, “Transport Phenomena Lecture 37 : Pseudocapacitors and batteries,” *ResearchGate*, pp. 1–12, 2011.

[20] H. Wang, J. Lin, and Z. Xiang, “Journal of science : advanced materials and devices polyaniline (PANi) based electrode materials for energy storage and conversion,” *J. Sci. Adv. Mater. Devices*, vol. 1, no. 3, pp. 225–255, 2016.

[21] Z. Tang, C. Tang, and H. Gong, “A high energy density asymmetric supercapacitor from nano-architectured Ni (OH) 2 / carbon nanotube electrodes,” *Adv. Funct. Mater.*, vol. 22, no. 6, pp. 1272–1278, 2012.

[22] R. Jose *et al.*, “Supercapacitor electrodes delivering high energy and power densities,” *Mater. Proc.*, vol. 3, no. 1, pp. 48–56, 2016.

[23] G. Qu *et al.*, “A fiber supercapacitor with high energy density based on hollow graphene / conducting polymer fiber electrode,” *Adv. Mater.*, vol. 28, no. 19, pp. 3646–3652, 2016.

[24] B. Dyatkin, V. Presser, M. Heon, M. R. Lukatskaya, and M. Beidaghi, “Development of a green supercapacitor composed entirely of environmentally friendly materials,” *ChemSusChem*, vol. 6, no. 12, pp. 2269–2280, 2013.

[25] F. Estrany, E. Armelin, and D. David, “Towards sustainable solid-state supercapacitors : electroactive conducting polymers combined with,” *J. Mater. Chem. C*, vol. 4, pp. 1792–1805, 2016.

[26] V. Kuzmenko, A. Bhaskar, H. Staaf, P. Lundgren, and P. Enoksson, “Sustainable supercapacitor components from cellulose,” *IEEE Trans. Ind. Informatics*, vol. 9, pp. 5–7, 2015.

[27] B. H. Robinson, “Science of the total environment e-waste : an assessment of global production and environmental impacts,” *NCBI*, vol. 408, no. 2, pp. 183–191, 2009.

[28] H. Cheng and I. Introduction, “Inorganic dissolvable electronics : materials and devices for biomedicine and environment,” *J. Mater. Res.*, vol. 31, no. 17, pp. 2549–2570, 2017.

[29] Y. H. Jung *et al.*, “High performance green flexible electronics based on biodegradable cellulose nanofibril paper,” *Nat. Commun.*, vol. 6, pp. 1–11, 2015.

[30] B. H. Kim *et al.*, “Dry transient electronic systems by use of materials that sublime,” *Adv. Funct. Mater.*, vol. 27, no. 12, 2017.

[31] S. P. Nichols, “Biocompatible materials for continuous glucose monitoring devices,” *Natl. Institutes Heal.*, vol. 113, no. 4, pp. 2528–2549, 2014.

[32] L. Sha, “Bio-compatible materials for advanced energy storage devices towards biomedical implantation,” *Res. Online*, 2014.

[33] B. Polyetherimide, M. Rajagopalan, I. Oh, R. Smalley, and R. Curl, “Fullerenol-based electroactive artificial muscles utilizing biocompatible polyetherimide,” *NCBI*, vol. 5, no. 3, pp. 2248–2256, 2011.

[34] Alan J Heeger, “The Nobel Prize in Chemistry , 2000 : Conductive polymers,” *R. Swedish Acad. Sci.*, pp. 1–16, 2000.

[35] A. González, E. Goikolea, J. Andoni, and R. Mysyk, “Review on supercapacitors : technologies and materials,” *Elsevier*, vol. 58, pp. 1189–1206, 2016.

[36] P. BioLabs, “Assessing Biocompatibility,” 2009.

[37] Y. Shi *et al.*, “Nanostructured conductive polymer gels as a general framework material to improve electrochemical performance of cathode materials in Li-Ion batteries,” *NANO Lett.*, vol. 17, no. 3, pp. 1906–1914, 2017.

[38] F. Li, Y. Wu, J. Chou, M. Winter, and N. Wu, “A mechanically robust and highly ion-conductive polymer - blend coating for high-power and long-life lithium-ion battery anodes,” *Adv. Mater.*, vol. 27, no. 1, pp. 130–137, 2015.

[39] A. J. T. Teo, A. Mishra, I. Park, Y. Kim, W. Park, and Y. Yoon, “Polymeric biomaterials for medical implants and devices,” *ACS Biomater.*, vol. 2, no. 4, pp. 454–472, 2016.

[40] R. Ravichandran and S. Sundarrajan, “Applications of conducting polymers and their issues in biomedical engineering,” *NCBI*, 2010.

[41] R. H. Warren, “Chapter 1 : Introduction,” *Calif. Berkeley*, vol. PhD Disser, 2015.

[42] A. J. Bard, L. R. Faulkner, E. Swain, and C. Robey, *Fundamentals and Applications*. 2000.

[43] M. Cossutta, *Life Cycle Analysis of Graphene in Supercapacitor Application*. 2016.

[44] C. Polo, D. S. Rosa, and S. Neves, “Development of a biodegradable polymer electrolyte for rechargeable batteries,” *J. Power Sources*, vol. 155, no. 2, pp. 381–384, 2006.

[45] M. Selvakumar and D. K. Bhat, “LiClO 4 doped cellulose acetate as biodegradable polymer electrolyte for supercapacitors,” *Appl. Polym. Sci.*, vol. 110, no. 1, pp. 594–602, 2008.

[46] C. P. Fonseca and S. Neves, “Electrochemical properties of a biodegradable polymer electrolyte applied to a rechargeable lithium battery,” *J. Power Sources*, vol. 159, no. 1, pp. 712–716, 2006.

[47] M. Y. S. Kalani *et al.*, “Food-materials-based edible supercapacitors food-materials-based edible supercapacitors,” *Adv. Mater. Technol.*, vol. 1, no. 3, 2016.

[48] C. Chen *et al.*, “All-wood, low tortuosity, aqeuous, biodegradable supercapacitors ultra-high capacitance,” *Energy Environ. Sci.*, vol. 10, p. 538, 2017.

[49] Y. Jo, W. Wu, S. Chun, J. F. Whitacre, and C. J. Bettinger, “Biologically derived melanin electrodes in aqueous sodium-ion energy storage devices,” *PNAS*, vol. 110, no. 52, pp. 20912–20917, 2013.

[50] M. Tsang, A. Armutlulu, A. W. Martinez, S. Ann, B. Allen, and M. G. Allen, “Biodegradable magnesium / iron batteries with polycaprolactone encapsulation : a microfabricated power source for transient implantable devices,” *Nature*, vol. 1, pp. 1–10, 2015.

[51] L. Wang, X. Li, and Y. Yang, “Preparation , properties and applications of polypyrroles,” *React. Funct. Polym.*, vol. 47, pp. 125–139, 2001.

[52] Y. Huang, H. Li, Z. Wang, M. Zhu, Z. Pei, and Q. Xue, “Nano energy nanostructured polypyrrole as a flexible electrode material of supercapacitor,” *Nano Energy*, vol. 22, pp. 422–438, 2016.

[53] K. Jurewicz, S. Delpeux, and V. Bertagna, “Supercapacitors from nanotubes / polypyrrole composites,” *Chem. Phys. Lett.*, vol. 347, no. 1–3, pp. 36–40, 2001.

[54] R. Buitrago-Sierra, M. J. García-Fernández, M. M. Pastor-blas, and A. Sepúlveda-escribano, “Green chemistry,” pp. 1981–1990, 2013.

[55] C. Dalmolin, S. R. Biaggio, N. Bocchi, and R. C. Rocha-filho, “Changes of electrochemical properties of polypyrrole when synthesized in a room-temperature ionic liquid,” *Mater. Chem. Phys.*, vol. 147, no. 1–2, pp. 99–104, 2014.

[56] L. Viau, J. Y. Hihn, S. Lakard, V. Moutarlier, V. Flaud, and B. Lakard, “Full characterization of polypyrrole thin films electrosynthesized in room temperature ionic liquids , water or acetonitrile,” *Electrochim. Acta*, vol. 137, pp. 298–310, 2014.

[57] V. Syritski, J. Reut, and K. Idla, “Environmental QCM sensors coated with polypyrrole,” *Synth. Met.*, vol. 102, pp. 1327–1327, 1999.

[58] Q. Ameer, “Polypyrrole-based electronic noses for environmental and industrial analysis and industrial analysis,” *Sensors Actuators B. Chem.*, vol. 106, pp. 541–552, 2005.

[59] K. M. Sajesh, R. Jayakumar, S. V Nair, and K. P. Chennazhi, “International journal of biological macromolecules biocompatible conducting chitosan / polypyrrole – alginate composite scaffold for bone tissue engineering,” *Int. J. Biol. Macromol.*, vol. 62, pp. 465–471, 2013.

[60] C. R. Broda, J. Y. Lee, S. Sirivisoot, C. E. Schmidt, and B. S. Harrison, “A chemically polymerized electrically conducting composite of polypyrrole nanoparticles and polyurethane for tissue engineering,” *NCBI*, vol. 98, no. 4, pp. 509–516, 2011.

[61] K. Arora *et al.*, “Application of electrochemically prepared polypyrrole – polyvinyl sulphonate films to DNA biosensor,” *Biosens. Bioelectron.*, vol. 21, pp. 1777–1783, 2006.

[62] Z. G. and L. G. Bingxi Yan, Boyi Li, Forest Zunecke, “Polypyrrole-based implantable electroactive pump for controlled drug microinjection,” *Appl. Mater. Interfaces*, vol. 7, pp. 14563–14598, 2015.

[63] J. P. M. J. Rodriguez, H. Grande, T.F. Otero, T. Trigaud, “Implanted polymer junctions from highly compacted polypyrrole films,” *Synth. Met.*, vol. 83, pp. 201–203, 1996.

[64] X. He *et al.*, “Transient resistive switching devices made from egg albumen dielectrics and dissolvable electrodes,” *Appl. Mater. Interfaces*, vol. 8, pp. 10954–10960, 2016.

[65] M. Singh, P. K. Kathuroju, and N. Jampana, “Chemical polypyrrole based amperometric glucose biosensors,” *Sensors Actuators B Chem.*, vol. 143, pp. 430–443, 2009.

[66] V. Janaki and S. Kamala-Kannan, “Environmental Applications of Polypyrrole- and Polyaniline-Bacterial Extracellular Polysaccharide Nanocomposites,” in *Eco-friendly Polymer Nanocomposites: Chemistry and Applications*, V. K. Thakur and M. K. Thakur, Eds. New Delhi: Springer India, 2015, pp. 387–397.

[67] S. Y. Yu Q, Xu S, Zhang K, “Multi-porous electroactive poly(L-lactic acid)/polypyrrole composite micro/nano fibrous scaffolds promote neurite outgrowth in PC12 cells,” *Neural Regen. Res.*, pp. 31–38, 2013.

[68] P. M. George *et al.*, “Fabrication and biocompatibility of polypyrrole implants suitable for neural prosthetics,” *Biomaterials*, vol. 26, pp. 3511–3519, 2005.

[69] T. Royal, S. Interface, H. Navsaria, Q. Mary, P. Vadgama, and Q. Mary, “Polypyrrole-based conducting polymers and interactions with biological tissues polypyrrole-based conducting polymers and interactions with biological

tissues," *R. Soc. Publ.*, vol. 3, no. 11, pp. 741–752, 2007.

[70] A. N. Zelikin, D. M. Lynn, J. Farhadi, I. Martin, V. Shastri, and R. Langer, "Erodible conducting polymers for potential biomedical applications," *Angew. Chemie*, vol. 41, no. 1, pp. 141–144, 2002.

[71] P. Chandrasekhar, *Conducting Polymers, Fundamentals and Applications: A Practical Approach*. 1999.

[72] P. Kar, "Doping in conjugated polymers," 2013.

[73] M. Zhou and È. Heinze, "Electropolymerization of pyrrole and electrochemical study of polypyrrole : evidence for structural diversity of polypyrrole," vol. 44, pp. 1733–1748, 1999.

[74] R. Warren, F. Sammoura, K. S. Teh, A. Kozinda, X. Zang, and L. Lin, "Electrochemically synthesized and vertically aligned carbon nanotube - polypyrrole nanolayers for high energy storage devices," *Sensors Actuators A Phys.*, vol. 231, pp. 65–73, 2015.

[75] L. Fan and J. Maier, "High-performance polypyrrole electrode materials for redox supercapacitors," *Electrochem. Commun.*, vol. 8, pp. 937–940, 2006.

[76] X. Zang *et al.*, "Evaluation of layer-by-layer graphene structures as supercapacitor electrode materials," *J. Appl. Phys. 115*, vol. 24305, no. 115, 2014.

[77] J. Chen *et al.*, "Facile co-electrodeposition method for high-performance supercapacitor based on reduced graphene oxide / polypyrrole composite film," *Appl. Mater. Interfaces*, 2017.

[78] Z. Peng, J. Lin, R. Ye, E. L. G. Samuel, and J. M. Tour, "Flexible and stackable laser-induced graphene supercapacitors," *Appl. Energy*, vol. 7, pp. 3414–3419, 2015.

[79] Gamry Instruments, "Equivalent circuit modeling using the Gamry EIS300 electrochemical impedance spectroscopy software," *Gamry Publications*, 2015.

[80] A. K. Serkan Junyi Shen, Alireza Dusmez, "Optimization of sizing and battery cycle life in battery/ultracapacitor hybrid energy storage systems for electric vehicle applicaitons," *IEEE Trans. Ind. Informatics*, vol. 10, no. 4, pp. 2112–2121.

[81] S. B. D. R.K. Sharma, A.C. Rastogi, "Manganese oxide embedded polypyrrole nanocomposites for electrochemical supercapacitor," *Electrochim. Acta*, vol. 53, no. 26, pp. 7690–7695, 2008.

[82] M. Stoller and R. Ruoff, "Best practice methods for determining an electrode material's performance for ultracapacitors," *Energy Environ. Sci.*, vol. 3, pp. 1294–1301, 2010.

[83] R. Muller, “Volummetric changes,” *Adv. Mater.*, vol. 11, no. 11, 1999.

[84] A. Thess *et al.*, “Crystalline ropes of metallic carbon nanotubes,” *Am. Assoc. Adv. Sci.*, vol. 273, no. 5274, pp. 483–487, 2017.

[85] C. Journet, W. K. Maser, P. Bernier, and A. Loiseau, “Large-scale production of single-walled carbon nanotubes by the electric-arc technique,” *Lett. to Nat.*, vol. 388, no. August, pp. 20–22, 1997.

[86] C. A. Poland *et al.*, “Carbon nanotubes introduced into the abdominal cavity of mice show asbestos- like pathogenicity in a pilot study,” pp. 423–428, 2008.

[87] D. A. Links, A. Bianco, K. Kostarelos, and M. Prato, “Making carbon nanotubes biocompatible and biodegradable,” *ChemComm*, pp. 10182–10188, 2011.

[88] M. J. O. Connell *et al.*, “Reversible water-solubilization of single-walled carbon nanotubes by polymer wrapping,” vol. 342, pp. 265–271, 2001.

[89] S. Bellucci, “Carbon nanotubes toxicity,” *Nanoparticles Nanodevices Biol. Appl.*, pp. 47–67, 2009.

[90] Y. Liu, Y. Zhao, B. Sun, and C. Chen, “Understanding the toxicity of carbon,” *Acc. Chem. Res.*, vol. 46, no. 3, pp. 702–713, 2013.

[91] S. Y. Madani, A. Mandel, and A. M. Seifalian, “A concise review of carbon nanotube’s toxicology,” *Nano Rev.*, vol. 4, pp. 1–14, 2013.

[92] K. B. K. Teo, M. Chhowalla, and W. I. Milne, “Catalytic synthesis of carbon nanotubes and nanofibers,” *Encyclopedia of Nanoscience and Nanotechnology*. pp. 1–22, 2003.

[93] T. Abitbol *et al.*, “Nanocellulose , a tiny fiber with huge applications,” *Sci. Direct*, vol. 39, no. I, pp. 76–88, 2016.

[94] M. B. and G. Westman, *Crystalline Nanocellulose — Preparation , Modification*. 2015.

[95] J. Adamcik, S. Handschin, C. Schu, I. Usov, G. Nystro, and A. Fall, “Fibril level,” *Nat. Commun.*, vol. 6, 2015.

[96] R. Sabo, A. Yermakov, C. T. Law, R. Elhajjar, U. F. Service, and G. Pinchot, “Nanocellulose-enabled electronics , energy harvesting devices , smart materials and sensors : a review,” *Scrivener Publ. LLC*, vol. 4, no. 5, pp. 297–312, 2016.

[97] A. Abenoja *et al.*, “Analytica chimica acta graphene-based field effect transistor in two-dimensional paper networks,” *Anal. Chim. Acta*, vol. 917, pp. 101–106, 2016.

[98] Y. Zheng, Z. He, Y. Gao, and J. Liu, “Direct desktop printed-circuits-on-paper flexible electronics,” *Sci. Rep.*, vol. 3, no. 1786, pp. 1–7, 2013.

[99] X. Zeng, L. Deng, Y. Yao, and R. Sun, “Flexible dielectric papers based on biodegradable cellulose nanofibers and carbon nanotubes for dielectric energy storage †,” *J. Mater. Chem. C*, vol. 4, pp. 6037–6044, 2016.

[100] F. Hoeng and J. Bras, “Use of nanocellulose in printed electronics,” *R. Soc. Chem.*, vol. 8, pp. 13131–13154, 2016.

[101] C. Paper, “Sampo Tuukkanen , Farzin Jahangiri and Sami Franssila,” no. 16, 2015.

[102] A. H. Bhat, A. Abu, and B. Universiti, “Cellulosic nanocomposites from natural fibers for medical applications: a review,” *Res. Gate*, no. 56, 2014.

[103] Cherian B.M. et al, “Bacterial nanocellulose for medical implants,” *Thomas S., Visakh P., Mathew A. Adv. Nat. Polym. Adv. Struct. Mater.*, vol. 18, 2013.

[104] Y. Lu, H. L. Tekinalp, C. C. Eberle, and W. Peter, “Nanocellulose in polymer composites and biomedical applications,” *Nanocellulose*, vol. 13, no. 6, pp. 14–17, 2014.

[105] L. Tian, Q. Jiang, K. Liu, J. Luan, and R. R. Naik, “Bacterial nanocellulose-based flexible surface enhanced raman scattering substrate,” *Adv. Mater.*, vol. 3, pp. 1–8, 2016.

[106] Z. Wang *et al.*, “Surface modified nanocellulose fibers yield conducting polymer-based flexible supercapacitors with enhanced capacitances,” *ACS Nano*, vol. 9, no. 7, pp. 7563–7571, 2015.

[107] P. Tammela *et al.*, “Asymmetric supercapacitors based on carbon nanofibre and polypyrrole/nanocellulose composite electrodes,” *RSC Adv.*, vol. 5, no. 21, pp. 16405–16413, 2015.

[108] W. Hu, S. Chen, Z. Yang, L. Liu, and H. Wang, “Flexible electrically conductive nanocomposite membrane based on bacterial cellulose and polyaniline flexible electrically conductive nanocomposite membrane based on bacterial cellulose and polyaniline,” *J. Phys. Chem. B*, vol. 115, no. 26, pp. 8453–8457, 2011.

[109] G. Zu, J. Shen, L. Zou, F. Wang, and X. Wang, “Nanocellulose-derived highly porous carbon aerogels for supercapacitors,” *Carbon N. Y.*, vol. 99, pp. 203–211, 2016.

[110] X. Yang, K. Shi, I. Zhitomirsky, and E. D. Cranston, “Cellulose nanocrystal aerogels as universal 3D lightweight substrates for supercapacitor materials,” *Adv. Mater.*, vol. 27, no. 40, pp. 6104–6109, 2015.

[111] Y. Wang, “Flexible supercapacitors based on paper substrates : a new paradigm for low-cost energy storage,” *Chem. Soc. Rev.*, vol. 44, pp. 5181–5199, 2015.

[112] J. O. Z. Universit, A. T. Nanorods, E. P. C. View, and J. O. Zoppe, *Surface Modification of Nanocellulose Substrates*. 2014.

[113] A. J. Bard and L. R. Faulkner, *Electrochemical Methods Fundamentals and Applications*, 2nd ed. John Wiley & Sons, Inc., 2001.